Distributions and size scalings for strength in a one-dimensional random lattice with load redistribution to nearest and next-nearest neighbors

S. Leigh Phoenix
Department of Theoretical and Applied Mechanics, Cornell University, Ithaca, New York 14853

Irene J. Beyerlein
Structure-Property Relations, Los Alamos National Laboratory, Los Alamos, New Mexico 87545

(Received 28 January 2000)

Lattice and network models with elements that have random strength are useful tools in explaining various statistical features of failure in heterogeneous materials, including the evolution of failure clusters and overall strength distributions and size effects. Models have included random fuse and spring networks where Monte Carlo simulation coupled to scaling analysis from percolation theory has been a common approach. Unfortunately, severe computational demands have limited the network sizes that can be treated. To gain insight at large size scales, interest has returned to idealized fiber bundle models in one dimension. Many models can be solved exactly or asymptotically in increasing size n, but at the expense of major simplification of the local stress redistribution mechanism. Models have typically assumed either equal load-sharing among nonfailed elements, or nearest-neighbor, local load-sharing (LLS) where a failed element redistributes its load onto its two nearest flanking survivors. The present work considers a one-dimensional fiber bundle model under tapered load sharing (TLS), which assumes load redistribution to both the nearest and next-nearest neighbors in a two-to-one ratio. This rule reflects features found in a discrete mechanics model for load transfer in two-dimensional fiber composites and planar lattices. We assume that elements have strength 1 or 0, with probability p and $q=1-p$, respectively. We determine the structure and probabilities for critical configurations of broken fibers, which lead to bundle failure under a given load. We obtain rigorous asymptotic results for the strength distribution and size effect, as $n\to\infty$, with precisely determined constants and exponents. The results are a nontrivial extension of those under LLS in that failure clusters are combinatorially much more complicated and contain many bridging fibers. Consequently, certain probabilities are eigenvalues from recursive equations arising from the structure of TLS. Next-nearest neighbor effects weaken the material beyond what is predicted under LLS keeping only nearest neighbor overloads. Our results question the validity of scaling relationships that are based largely on Monte Carlo simulations on networks of limited size since some failure configurations appear only in extremely large bundles. The dilemma has much in common with the Petersburg paradox.

PACS number(s): 05.40.−a, 62.20.Mk

I. INTRODUCTION

A. Background

The size effect in the strength of brittle materials has been known since the time of Leonardo da Vinci (ca. 1500) who observed that wires weaken with increasing length [1], and in perhaps the first published work on the subject [2] Galileo noted that the strength of geometrically similar structures decreases as the dimensions increase. Fifty years ago Weibull [3,4] presented a statistical theory built on weakest-link concepts coupled with statistical variation in small volume elements representing the links. For a material under constant stress level x over volume $\mathcal{V}$, he proposed that its strength, X, has the cumulative distribution function

$$F(x)=1-\exp[-(\mathcal{V}/\mathcal{V}_0)(x/x_0)^{\rho}],\quad x\geqslant 0, \tag{1}$$

where ρ is the shape parameter, and x_0 is the scale parameter measured at reference volume $\mathcal{V}_0$.

In Weibull's model the strength scales algebraically with volume following $x_0\mathcal{V}^{-1/\rho}$. In this and other models [5,6], the resulting form of the distribution for strength and its size scaling depends strongly on the assumed functional form for the strength of small volume elements at low failure probabilities. Physically, such elements are often viewed as small enough to contain at most one cracklike flaw, where variation in the flaw size gives rise to variation in the strength of the element, and hence, overall material strength [7]. However, a firm foundation for specifying the form of the strength distribution in the high reliability regime (apart from mathematical scaling arguments [6]) has proven elusive both from physical fundamentals and experimental observations.

Brittle materials, such as monolithic ceramics, are actually heterogeneous when viewed at the microscale, often containing nonuniform distributions of grain shapes and sizes with flaws of various types at their boundaries (such as voids, inclusions, and microcracks). Failure often results from the local interaction and coalescence of several smaller flaws, rather than just the catastrophic growth of just one. Therefore identification of a ''critical flaw'' after failure (not to mention before) is extremely problematic. Moreover, many advanced materials are multiphase, with the potential to design their microstructure to enhance strength, toughness, and reliability. Experimentally achieving such improvements

by ''trial and error'' has proven costly, so that attention has turned to modeling of the failure process. Obtaining a good theoretical description of this process has required delving into microstructural and statistical details of the interaction of the various flaw features [8], and this has proven to be a deceptively difficult task.

One approach to accounting for such detail has been to develop discrete network or lattice models of the failure process. Early work in the engineering literature has borrowed from the classic work of Daniels [9] on simple fiber bundles under equal load sharing (ELS) among nonfailed fibers. Material failure models have often assumed a chain-of-bundles structure [10,11,12], with m bundles in series, and where the length of a single bundle is the characteristic length for fiber load transfer (often a few fiber diameters in magnitude). The material fails when the weakest bundle fails. Though analytically tractable, these ''mean field'' models and their global load-sharing (GLS) generalizations [13,14] are more applicable to the strength of weakly-bonded, fibrous materials than to tightly-bonded materials, which display more localized breakdown and flaw sensitivity. In the strength of small bundles, mild size effects exist [11,14] as the number of fibers n increases, but convergence of the strength to a finite, nonzero limit is rapid since the variability in strength decays as $1/\sqrt{n}$. Likewise the sensitivity of material strength to increasing chain length m rapidly diminishes as n increases.

Study of the failure of fiber-reinforced composites with strong, well-bonded, elastic matrices has led to another branch of network models, where the load-sharing is much more localized [15–22]. A chain-of-bundles framework is also commonly used. The basic fiber elements are often assumed to follow Eq. (1), but failed elements are assumed to redistribute their loads locally onto unfailed neighbors, increasing their probabilities of failure and thus the likelihood of a catastrophic cascade across the bundle. Rendering these models analytically tractable has required highly idealized assumptions in the form of load-sharing ''rules'' on the local load redistribution mechanism in a bundle. One such model, called local load-sharing (LLS) assumes that the loads of failed fibers are shifted in equal portions onto the nearest, flanking survivors. For planar versions with one-dimensional bundle structure, various recursive [18,21,22] and asymptotic methods [17,19,20] have been used with success. One major result is that the distribution function, $G_n(x)$, for the strength X_n of a bundle containing a total of n fiber elements (X_n is the total bundle load divided by n) is given by a quasi-weakest-link form

$$G_n(x) \approx 1-[1-W(x)]^n \approx 1-\exp[-nW(x)], \quad x \geqslant 0, \tag{2}$$

where $W(x)$ is one minus the largest eigenvalue of a certain transition matrix describing probabilities for local failure configurations. Longer composites viewed as a chain of m such bundles follow the same distribution but with mn replacing n. Except for the simple discrete fiber strength distribution where a fiber has strength x_0 with probability p, and strength zero with probability $q=1-p$, precise analytical forms for $W(x)$ have remained elusive. Nevertheless, Smith [17,20] was able to argue that for fiber elements following Eq. (1) and LLS, the median strength x^* follows:

$$x^* \approx \frac{\rho 2^{1-1/\rho} x_0}{\log n}. \tag{3}$$

(Here and throughout the paper, log refers to the natural logarithm $\log_e$ or ln). Recent progress on LLS, GLS, and ELS models is summarized in Phoenix and Beyerlein [23].

In recent years, network or lattice models of material failure have received considerable attention in the statistical physics literature particularly in connection to percolation theory. Models have been developed to treat conductivity breakdown in random fuse networks [24–31], dielectric breakdown in materials with randomly dispersed conducting inclusions [31,32] critical currents in disordered superconducting networks [25,33,34], and catastrophic failure of elastic lattices with random element strength [35–38]. The random fuse model, introduced by de Arcangelis *et al.* [24], has become a useful prototypical model. Such network models often consider a planar square lattice of size $L \times L$, where the conducting elements are initially fuses with probability p or insulators with probability $q=1-p$. Of interest is the range $p > p_c$, where p_c is the percolation threshold, so that a large network is initially conducting. A voltage gradient v (the applied voltage normalized by L) is applied in the longitudinal dimension, and calculation of the currents in all the surviving fuses is done through numerical solution of Kirchoff's laws. Each fuse has constant resistance when the calculated voltage across it is less than a critical value v_c, but burns out to become an insulator when its voltage exceeds v_c.

Monte Carlo simulations on sample fuse networks have been carried out [24,27] under a continually increasing voltage gradient to empirically determine the respective distributions of the gradient V_1 that fails the initially ''hottest'' fuse, and the gradient V_b when a catastrophic ''crack'' finally severs the material. Because of the computational demands, results have been generated only for relatively small lattices up to about 200×200. Results show a difference between the mean values of V_1 and V_b and their dependence on size L^2. For the most homogeneous networks (p near 1), $V_1 \approx V_b$ as the failure process appears to be self-sustaining after the first bond failure.

Duxbury *et al.* [27] noticed anomalous scaling (i.e., different from that found in percolation theory) in the two breakdown voltages V_1 and V_b, which were seen to continually decrease with increasing network size with no apparent positive lower bound. To explain this size dependence they considered Lifshitz-type arguments on the effect of a ''defect cluster'' in a large lattice in the form of a contiguous transverse row of missing fuse elements, focusing on the current enhancement at the row tips. They attempted to determine the statistics of the largest *critical* defect cluster in the lattice in the dilute limit (p near 1). They assumed that the most critical defect would be the one with the most current enhancement, namely a transverse slit or ''crack.'' Using a continuum approach involving the solution to Laplace's equation they determined the current enhancements $\tilde{i}_{\mathrm{tip}} \sim \tilde{i}(1+k^*\sqrt{j})$ where j is the number of adjacent missing fuses in the defect cluster, $\tilde{i}$ is the externally applied current to the network per unit width and k^* is a constant. They also appreciated the importance of defect cluster geometry whereby current enhancement was proposed to be approxi-

mately proportional to j (rather than $\sqrt{j}$) when a single intact fuse bridges two adjacent collinear defect clusters of size $j/2$. Li and Duxbury [29] later revised this dependence to $\tilde{i}_{\mathrm{tip}} \sim \tilde{i} j/\log j$. In such configurations, failure of the bridging fuse caused the two clusters to coalesce forming a larger cluster of size $j+1$ but with lower current enhancement at its edges than was in the bridging fuse. Thus, an even larger external voltage is needed to fail the network. Consequently V_1 and V_b would have different scaling behavior.

A key analytical step by Duxbury *et al.* [27] was to estimate the probability that no cluster of $j+1$ or more transversely adjacent fuses will be missing *anywhere* in the $L \times L$ network obtaining $(1-pq^{j+1})^{L^2} \sim \exp[-pqL^2 \exp(-jk)]$, where $k=-\log q$. Appealing to the statistical theory of extremes, they then argued that the distribution functions for the normalized breakdown voltages V_1 and V_b, respectively, must have the forms (in 2D)

$$G_{L^2}(v_s) = 1 - \exp[-c_s L^2 \exp(-k_s v_s^{-1/\alpha_s})], \quad s = 1, b, \quad (4)$$

where c_s and k_s are constants depending on p, and α_s is an exponent independent of p. They recognized the difficulties in obtaining analytical expressions for the various constants and exponents for general p. However, for the dilute case of p near one (or $0<q\ll 1$) the above arguments suggested $\alpha_1 \approx 1$, $k_1 \approx -\log q$ and $c_1 \approx pq$ for V_1, and $\alpha_b \approx 1/2$ and $k_b \propto -\log q$, for V_b. The size effect for the breakdown voltages, obtained by solving $G_{L^2}(v_s^*) = 1/2$ in Eq. (4), yielded the median

$$v_s^* = 1/[A_s(p) + B_s(p) \log L]^{\alpha_s}, \quad s = 1, b, \quad (5)$$

where $A_s(p) = (\log c_s - \log \log 2)/k_s$, and $B_s(p) = 2/k_s$. For $s=1$, Eq. (5) is asymptotically of the same form as Eq. (3). The above distributional form and size effects in V_1 and V_b were largely supported by Monte Carlo simulations of networks up to 200×200 in size [27].

Similarly, in studies of network models of dielectric breakdown in metal-loaded dielectrics [31,32], and elastic failure in a two-dimensional triangular lattice [36], the analogous initial and final breakdown fields and size effects were argued to have forms Eqs. (4) and (5), and the critical defect was argued to be an arrangement of two close collinear failure clusters. On the contrary, for the initial and final breakdown fields it was argued that this type of defect leads to *equivalent* rather than different distributional forms and size effects, as was supported by Monte Carlo simulations on networks of limited size.

The general size scalings and distributional forms described above have not always been apparent from simulations in spring networks [35,37,39,40]. Further increasing the disorder in a network through randomizing the elastic spring stiffnesses [35] may increase dispersion in the load redistribution, thus driving the network away from LLS-like behavior towards ELS or GLS behavior, especially at smaller size scales. This may mask the emergence of the ultimate large scale LLS behavior. Various continuous distributions for element strength X have also been used, as described by Hansen [39] who discussed results under the probability density function of the power form $\hat{p}(x) = (1-\alpha)x^{-\alpha}$ for $0 < x \leq 1$ and α near 1. These forms appeared to have scalings similar to those in percolation, rather than Eqs. (3) and (5). On the other hand Hansen *et al.* [37] assumed a continuous, uniform distribution $\hat{p}(x) = 1$ for $0 < x \leq 1$, and argued for power-law scaling in applied force per unit width, $F_{\max}/L \propto L^{\beta-1}$, where $\beta = 3/4$. In fact $\beta = 3/4$ was argued to be insensitive to the choice of $\hat{p}(x)$. They suggested that disagreement with the scaling of Eq. (5) results from the difference in assumptions on the form of $\hat{p}(x)$, which in the case of Eq. (5) is distinctly discrete with only two possible strengths, 0 or 1; that is $\hat{p}(x) = p\,\delta(x-1) + q\,\delta(x)$ where δ is a Dirac delta function. In later work, Hansen *et al.* [40] argued that for $p > p_c$, rescaling through a renormalization argument leads to the disappearance of disorder as the effective value of p, defined at scale L, converges to 1 as $L \to \infty$. Thus such models were thought to be asymptotically equivalent to a disorderless system which would have a *finite* average strength in an infinite lattice limit, and so, observations of the form of Eq. (5) were suggested to be transient effects. Perhaps the main origin of the controversy over the particular form of the size scaling is that simulations covering many orders of magnitude in sample dimensions are necessary to arrive at definitive conclusions on the size effect. In most cases, such sizes have been inaccessible by Monte Carlo simulation alone as lattices approaching 1000×1000 in size rapidly become too demanding computationally. The model developed in this paper will show that lattices of even this computationally formidable size are often much too small to reveal the ultimate large scale behavior. This is an important issue since real structural components, such as fibrous composite pressure vessels or bridge cables, may have from 10^8 to 10^{16} fiber elements.

Regardless of their points of view, many investigators have turned to rigorous study of idealized, one-dimensional models of failure [41–48] in an attempt to put approximate analyses and interpretations from simulations of more complex networks on firmer ground. Such models, which are often variations on the LLS models of Harlow and Phoenix [18,41], are analytically solvable, rich in behavior, and qualitatively show the many features seen in simulations. In most cases, results in LLS fiber bundle models support the logarithmic size scaling in Eqs. (3) and (5), but more generally, such results depend on the load-sharing scheme (LLS vs ELS) and on the assumed form of the distribution for element failure. For example, in an LLS setting involving time-dependent breakdown of elements, Curtin and Scher [49,50] analytically uncovered transitions from scaling as in Eqs. (3) and (5) to ELS-type scaling as $L \to \infty$, simply by changing the value of a distribution parameter. Subtle scalings and transitions have also been noticed in fiber bundle models with heirarchical load-sharing as discussed in Newman *et al.* [51] and references therein.

B. Overview of paper and main results

This paper continues the study of series-parallel models in two dimensions with the basic analytical structure of one-dimensional load sharing. The LLS model is modified to a more diffuse tapered load-sharing (TLS) rule whereby 2/3 of the load of a failed fiber is redistributed equally onto the nearest unfailed neighbors and 1/3 is redistributed equally to

the next nearest unfailed neighbors, except when a fiber is surrounded by breaks whereby it takes half the shed load coming from each side. Again we assume that fibers have strength 1 with probability p and strength 0 with probability $q=1-p$. We motivate the key aspects of the load-sharing rule in the context of aligned fibrous composites through use of results for transverse patterns of aligned fiber breaks in the classic shear-lag model of Hedgepeth [52–57], which also turn out to be characteristic of elastic lattice models. One focus will be to determine the structure and probabilities for critical failure configurations with a view towards determining the extent to which the most critical defects are single clusters, or double clusters separated by a single intact fiber, or much more complicated configurations. We will also investigate the extent to which the load at first element failure scales as the load at final failure. Though the detailed calculations are tedious, the model is solvable asymptotically as the bundle size n increases. Thus we obtain precise asymptotic results for the various distributions and size scalings, giving error estimates and rates of convergence as $n\to\infty$ and $x\to 0$. In particular, we are able to evaluate all the constants in the model in terms of the total number of fibers n (the volume), and p and q and the TLS rule.

The analysis is based on the Chen-Stein method of Poisson approximation as described in Arratia *et al.* [58] and Barbour *et al.* [59] and used earlier by Harlow and Phoenix [41] for LLS bundles. These problems have a strong connection to probabilities for long head runs in coin tossing experiments [60]. The key idea is to determine all possible local failure configurations with sufficient detail to render them suitably distinct. Such problems have a history of being difficult. In fact, the dramatic differences between expectation and realized outcome have provided the basis for the historical Petersburg paradox [61,62].

The remainder of the paper is organized as follows: In Sec. II we describe the behavior of load redistribution in the model of Hedgepeth. In Sec. III we idealize the key features seen in Sec. II to describe the tapered load-sharing rule for a 1D bundle of n fibers, and the relationship between the bundle strength and the load-sharing constants in the failure configurations that arise. In Sec. IV we gain experience by studying the various local failure configurations and their probabilities, which are associated with bundle failure at loads x in the range $1/3<x\leqslant 1$. In Sec. V we build on this experience and describe the general structure of the local failure configurations for $0<x\leqslant 1$. In Sec. VI we present expressions for the probabilities of occurrence of the dominant failure configurations obtained in Sec. V at any given location in the bundle. In Sec. VII we study the asymptotic structure of these probabilities as the bundle load x becomes smaller, which is relevant to very large bundles. In Sec. VIII we use the Chen-Stein theorem to develop key results that allow us to estimate the distribution function for bundle strength, $G_n(x)$. In the analysis we pay particular attention to errors of approximation *relative* to $G_n(x)$. We show that these errors become negligible as the bundle size n increases and x decreases.

In Sec. IX we study the dependence of the bundle strength on n taking special care to evaluate the error terms. In particular we show that bundle strength X_n satisfies $X_n\sim -\log\hat{q}/\log n$ in probability as $n\to\infty$ where $\hat{q}=q^2\delta$ and where δ solves the characteristic equation $\delta^2-q\delta+q(1-q)=0$ arising from certain key failure configurations. In fact, $\delta\approx\sqrt{q}+q/2$ for small q. In Sec. X we consider the behavior of the cumulative distribution function $G_n(x)$ for the bundle strength, and determine the approximation

$$G_n(x)\approx 1-\exp\left\{-n\Pi^*(q)\Delta(1/x)\left(\frac{1}{x}\right)^2\times\exp\left[-(-\log\hat{q})\left(\frac{1}{x}\right)\right]\right\},\quad x>0,$$

where $\Pi^*(q)$ is a known constant and $\Delta(1/x)$ is a known function that is asymptotically periodic in $1/x$ as $x\to 0^+$.

On the other hand, the load at first fiber failure, $X_n^{(1)}$, follows $X_n^{(1)}\sim -2\log q/\log n$ as $n\to\infty$, and thus, scales differently from the bundle strength, X_n. An approximation for the cumulative distribution function $G_n^{(1)}(x)$ for $X_n^{(1)}$ is found to be

$$G_n^{(1)}(x)\approx 1-\exp\left\{-n(p/q)^2\Delta^{(1)}(2/x)\left(\frac{2}{x}\right)\times\exp\left[-(-\log q)\left(\frac{2}{x}\right)\right]\right\},\quad x>0,$$

where $\Delta^{(1)}(2/x)$ is asymptotically periodic in $2/x$ as $x\to 0^+$, varying between 1 and q.

In Sec. XI we discuss extensions to chain-of-bundle structures applicable to 2D. We also consider how the bundle strength will behave when other important features of the Hedgepeth load-sharing model are taken into account such as the growth in load concentration with the square-root of the size of the failure cluster.

In all, when we draw the correspondence between the breakdown voltages V_1 and V_b in the random fuse network given by Eqs. (4) and (5) and the bundle strengths $X_n^{(1)}$ and X_n in the TLS bundle model, we find that the distributions and scalings are much more complicated than represented by Eqs. (4) and (5) of earlier work. We also see that the eventual size scaling emerges only for extremely large networks. This points to the pitfalls in expecting Monte Carlo simulation of networks of limited size to reveal the true large scale behavior.

II. HEDGEPETH LOAD-REDISTRIBUTION MODEL

To motivate our fiber load-sharing rule we review briefly some results from the classic micromechanics model developed by Hedgepeth [52] and extended by others [53–57]. The results are for load concentrations in fibers near multiple broken fibers in a unidirectional, planar composite sheet, and we also present some new results for multiple collinear clusters or ''cracks'' of various separations and sizes. In the Hedgepeth model the equispaced fibers are elastic, deform and carry loads only in tension, and are well-bonded to the matrix. The matrix is also elastic but deforms and carries load only in simple shear, and thus, is the vehicle for transmitting the tensile load of a broken fiber to its intact neighbors. These are the classic shear-lag assumptions in elastic-

ity, which work well when the elastic shear modulus of the matrix is much smaller than the Young's modulus of the fibers. The 2D Hedgepeth model is discrete in the transverse dimension but continuous in the longitudinal dimension, as compared to a fully discrete square elastic network with longitudinal tensile springs and transverse shear springs. In the latter, lattice Green function methods have been used to determine load concentrations around broken elements [63–65]. It can be shown that the Hedgepeth model is a natural continuous limit of these 2D lattice models when the ratio of the transverse element shear stiffness to longitudinal extensional stiffness goes to zero but with longitudinal distance rescaled through maintaining a fixed characteristic length of longitudinal load transfer [23,65]. An electrical analogy of the Hedgepeth model [66] involves thin conducting wires in a weak electrolyte; near wire breaks, current enhancements are the analog of load enhancements and voltage drops of break opening displacements. This parallels the analogy between spring networks and random fuse networks. Recently, load and current concentrations in both discrete networks and the Hedgepeth model have been studied by Taylor and Sweitzer [67] and Taylor [68,69] by drawing a mathematical connection to random walk theory [70].

A. Load concentrations and connections with continuum fracture mechanics

Hedgepeth originally considered load concentrations produced by an aligned row of t contiguous fiber breaks transverse to the fiber and loading direction. The magnitudes of the load concentrations in unbroken fibers along the transverse plane of the breaks turn out to be independent of the stiffness moduli, spacings, and cross-sectional areas of the fibers and matrix (though the longitudinal length scale of load transfer depends on these quantities). For this row of t consecutive fiber breaks, let z be the count of an intact fiber away from the last break; that is, $z=1$ for the adjacent fiber, $z=2$ for the subadjacent fiber and so on. Best known is Hedgepeth's result (proven rigorously by Hikami and Chou [57]) for the peak load concentration $K(t,1)$ on the first intact fiber $(z=1)$ adjacent to the t-break cluster, which is

$$K(t,1)=\frac{(4)(6)\cdots(2t+2)}{(3)(5)\cdots(2t+1)}, \quad t=1,2,3,\ldots, \tag{6}$$

with $K(0,1)=1$. This evaluates to $K(1,1)=1.333$ and $K(2,1)=1.600$, $K(3,1)=1.829$, etc. More generally Hikami and Chou [57] determined that

$$K(t,z)=(t+2z-1)\times\frac{(2z)(2z+2)(2z+4)\cdots(2z+2t-2)}{(2z-1)(2z+1)(2z+3)\cdots(2z+2t-1)},$$

$$t,z=1,2,3,\ldots, \tag{7}$$

with $K(0,z)=1$. For $t=1$, Eq. (7) gives $K(1,z)=1+1/(4z^2-1)$ which yields $K(1,1)=4/3$ and $K(1,2)=16/15$. Note that the shifted load scales as $1/(4z^2)$ for larger z.

Beyerlein *et al.* [54] have favorably compared Eqs. (6) and (7) with elastic fracture mechanics results for a mode I central crack of length t in an infinite continuum sheet. An extremely accurate approximation to Eq. (6) with the correct asymptotics as $t\to\infty$, was found by Phoenix and Beyerlein [23] to be

$$K(t,1)\approx\sqrt{1+\pi t/4}. \tag{8}$$

They also showed that [23]

$$K(t,z)\approx K(t,1)\left[\frac{z}{(2z-1)K(z-1,1)}\right]\approx\frac{K(t,1)}{\sqrt{1+\pi(z-1)}}. \tag{9}$$

Both Eqs. (8) and (9) have small error though the latter requires $z\ll t$. Note that for $z=1$, 2, 3, and 4, the factor in square brackets takes the values 1, 1/2, 3/8, and 15/48, so for a large cluster of breaks, the load concentration on the next-nearest neighbor is only *half* that on the nearest neighbor. These asymptotic results are of the same form as the continuum results for the K-field at the tip of a crack [54], reflecting the continuum solution above the length scale of the fiber spacing. Thus the Hedgepeth model gives discrete results for loads surrounding a single transverse crack that are in close agreement with results from linear elasticity but without being singular. We note that in the discrete spring network with equal tensile and shear springs, the load concentrations, while having scaling in t and z similar to that in Eqs. (8) and (9), are less severe on the nearest neighbor [67,68], and slightly more severe on the next-nearest neighbor. For example, $K(1,1)=1.273$ versus 1.333, and $K(20,1)=3.737$ versus 4.088. For large t the difference is about 10%.

B. Load concentrations on bridging fibers

Previous discussion mentioned the important role of fiber elements bridging long clusters of breaks. We have constructed an accurate approximation for the load concentration $K(t_1,t_2,b)$ in a single fiber or an adjacent pair of fibers (ignoring minor differences in the two) lying between two collinear clusters of size t_1 and t_2 respectively. This approximation is

$$K(t_1,t_2,b)\approx\frac{2\sqrt{t_1t_2}(N+b)}{(t_1+t_2)b\left\{1+\frac{N+b}{4(N+2b)}+\frac{1}{\pi}\log\left[\frac{N(N+3b)}{2b(2N+b)}\right]\right\}}, \quad b=1,2, \text{ and } N=1,2,3,\ldots, \tag{10}$$

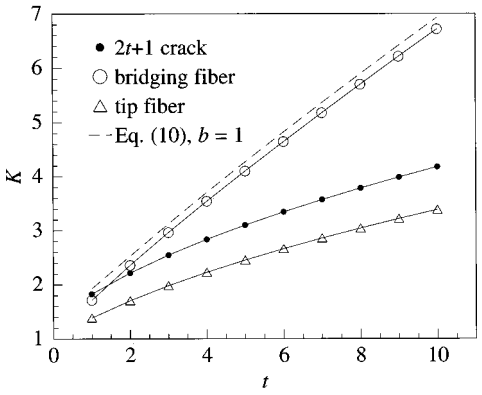

FIG. 1. Load concentrations predicted by the Hedgepeth model for two t-fiber break clusters separated by a single intact fiber, $b=1$, before and after its failure. Also shown is the analytical result, Eq. (10).

where $N=(t_1+t_2)/2$, $b=1,2$ is the number of consecutive bridging fibers, and $t_1,t_2 \gg 1$. When $t_1=t_2$, Eq. (10) has the same asymptotics as a result given in Taylor and Sweitzer [67] for a square lattice. For $t_1 \neq t_2$ Eq. (10) has the asymptotics $K(t_1,t_2,b) \sim \pi\sqrt{t_1 t_2}/\log(t_1+t_2)$ as pointed out by Taylor [69] who has mentioned a connection to results in Kesten [69] for random walks. However this last approximation is very inaccurate unless t_1 and t_2 are very large.

The good performance of Eq. (10) for $b=1$, as compared to numerical results, is seen in Fig. 1, which shows the load concentration in a lone intact ''bridging'' fiber between two t-fiber break clusters (open circles) and those in the fibers at the tips (triangles), respectively. Also shown is $K(2t+1,1)$ according to Eq. (6) for a $2t+1$ straight crack (solid circles) after failure of the bridging fiber. The key feature is that while the single bridging fiber effectively reduces the load concentration at the tip as compared to a $2t+1$ (and also $2t$) straight crack, it sustains a divergingly higher load concentration. For example, for $t=6$ (or 12 breaks in total), when the bridging fiber breaks under the load concentration of 4.65, the load concentration at the tips jumps from 2.66 to 3.35 for the new cluster of 13 breaks.

The good performance of Eq. (10) for $b=2$ is shown in Fig. 2, which shows numerical results for the load concentration in a pair of intact fibers ''bridging'' between two t-fiber break clusters (open circles), those in the fibers at the tips [triangles from Eq. (6)], as well as those at the tips of a single cluster of $2t+2$ contiguous breaks (solid circles), respectively. These two bridging fibers powerfully suppress the load concentrations at the tips as compared to the situation for a crack of $2t+2$ contiguous broken fibers. They also require a higher applied load to fail them than fibers at the tip of a fairly long *contiguous* cluster of nearly 20 fiber breaks. The opposite is true for $2t \geqslant 20$. Thus pairs of bridging fibers act as effective ''crack arrestors.'' It can be shown that a triplet of intact bridging fibers is even more effective and for much longer cracks.

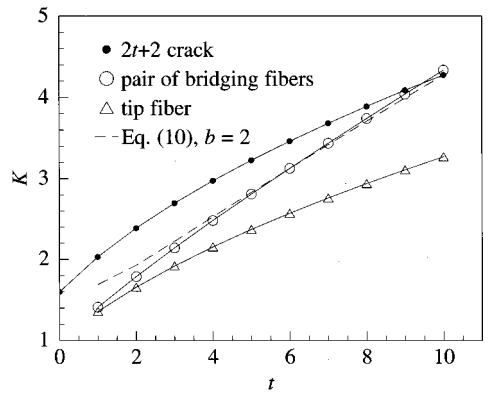

FIG. 2. Load concentrations predicted by the Hedgepeth model for two t-sized fiber break clusters separated by a pair of intact fibers, $b=2$, before and after their failure. Also shown is the analytical result, Eq. (10).

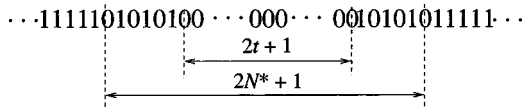

FIG. 3. Symmetric configuration of breaks corresponding to load calculations in Fig. 4.

A third important feature is that it is possible to spread $2N+1$ breaks over an extended $2N^*+1$ length such that this cluster is considerably weaker than a contiguous row of $2N+1$ adjacent breaks. This can be seen by considering a symmetric configuration of breaks arranged as shown in Fig. 3. There is a central core cluster of $2t+1$ contiguous breaks flanked on each side by $2(N-t)$ alternating intact and broken fibers, giving a total length $2t+1+4(N-t)=2[N+(N-t)]+1=2N^*+1$, so $N^*=N+(N-t)$. For $2N+1=21$ and 51, Fig. 4 plots, versus t, the ratio of the load concentration $K_c(2t+1)$ on the fiber at the edge of the $2t+1$ core (while embedded in the $2N^*+1$ configuration) over the load concentration $K(2N^*+1,1)$ at the tip of a full crack of $2N^*+1$ breaks, (representing the case in which all the bridging fibers have broken). When this ratio is equal to or greater than one, failure of the two fibers at the edge of the core (and all subsequent bridging fibers flanking them) occurs at a lower load than that required to cause catastrophic failure in a $2N^*+1$ contiguous crack. For example, the diluted configuration containing 21 (51) breaks, has the strength of a contiguous crack of about 26 (63) breaks, representing effectively a 25% expansion in length. This ar-

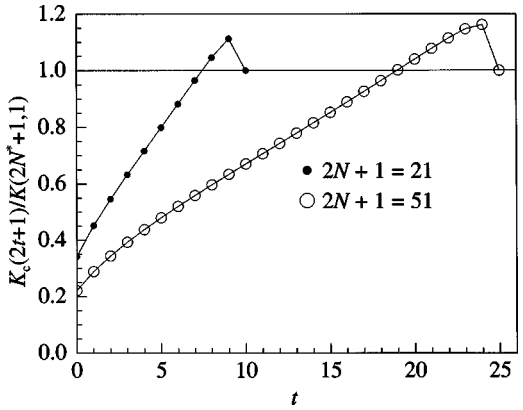

FIG. 4. Ratio of the load concentration in the nearest bridging fiber to a cluster of $2t+1$ breaks, shown in Fig. 3, to that in the first intact fiber ahead of a $2N^*+1$ straight crack, as calculated under the Hedgepeth model.

rangement of an initiating core cluster flanked with a diluted fringe of a few alternating bridging fibers, is by no means the weakest arrangement of $2N+1$ breaks that can be constructed. This is a key phenomenon seen in real materials, and is the theme of this paper.

C. Summary of important load redistribution features

The key points illustrated in these figures are as follows: First, isolated surviving fibers will fail at much lower loads than the cracks they become part of once broken. Second, configurations consisting of a core of contiguous breaks flanked by fringes of a few isolated bridging fibers will cause catastrophic failure at significantly lower loads than ''cracks'' consisting of either the same number or the same length of contiguous breaks. Third, isolated pairs of intact fibers act as crack arrestors for much longer break configurations surrounding them. One of the main tasks of this work will be to enumerate the probabilities for the preexistence of all the various types of such configurations that lead to composite failure at a given applied load. In Sec. III we develop an idealized tapered load-sharing rule which captures the three important features just described, but is amenable to rigorous analytical treatment, as shown in the remainder of this work.

III. TAPERED LOAD-SHARING RULE AND PARTITION OF THE LOAD RANGE

We now create an idealized rule called tapered load sharing (TLS), which is specifically designed to reflect the features of load redistribution in fibers as seen in Sec. II. The rule must allow us to analytically obtain the load concentration factors for all surviving fibers in *all* possible failure configurations, and it must lead to tractable analysis. Also, as a special case TLS should reduce to LLS of much earlier work [41–48].

A. Structure of TLS

First we consider a linear bundle with fibers numbered 1, 2, 3, . . . , n, from left to right. Then consider a surviving fiber that is adjacent to at least one other survivor, and that is directly adjacent to i contiguous fiber breaks (found only on one side) and is subadjacent to j fiber breaks, where $i,j \geqslant 0$. When $i=0$ and subadjacent breaks are found on both sides, j is the sum of both. For fixed θ satisfying $2/3 \leqslant \theta \leqslant 1$, the load concentration factor, $K_{i,j}$, on this survivor is given by

$$K_{i,j} = 1 + i\theta/2 + j(1-\theta)/2. \tag{11a}$$

On the other hand, for an *isolated* survivor adjacent to i contiguous breaks counting on both sides, the load concentration factor is given by

$$K_i^* = 1 + i/2. \tag{11b}$$

Otherwise a fiber's load-sharing constant is $K_{0,0}=1$. Thus, in Eq. (11a), a broken fiber shifts $\theta/2$ of its load to each of the closest survivors on each side and $(1-\theta)/2$ to each of the next closest survivors, which are directly adjacent to the closest survivors. If, however, the closest survivor is sandwiched by single breaks or rows of breaks on both of its sides, it takes 1/2 the shifted load of the broken fibers on both sides, as described by Eq. (11b). The special case of LLS is obtained by setting $\theta=1$ in Eq. (11), so that a failed fiber shifts half of its load onto each of its two flanking survivors. Also, in the case $\theta=2/3$ and for a single break, the fibers that are adjacent, subadjacent, and sub-subadjacent to this break have load concentration factors 4/3, 7/6, and 1, respectively, as compared to 4/3, 16/15, and 36/35 in the case of the Hedgepeth model, Eq. (7) where load is even more diffusely distributed. Note also that when $\theta=2/3$ and there is a large isolated cluster of i breaks, the load on the adjacent fiber is approximately double that on the subadjacent fiber in keeping with the behavior mentioned after Eq. (9).

The tapered load-sharing rule we have devised does not reflect some of the features in the Hedgepeth model of Sec. II, which are the result of longer range effects in load transfer. In particular, the load concentration on a fiber next to a large isolated cluster of i breaks does not have the square-root dependence on i, reflected in Eq. (8), but rather is linear in i. Nevertheless our TLS scheme can be revised to reflect such behavior provided that we are willing to neglect overloads beyond the next nearest neighors, although the loads in surviving fibers will no longer sum to the applied load. The effects of such an adjustment will be clear from the structure of the final results. Note that in interpreting random fuse and spring network simulation results, using analysis leading to Eqs. (4) and (5), loads shifted beyond nearest neighbors have been neglected in the past [27,31,32,36]. The present analysis represents a major step towards assessing the effects of such simplifications, which turn out to lead to considerable inaccuracies in prediction.

Denoting an intact fiber by ''1'' and a failed fiber by ''0'' we show a few possibilities below:

$$\begin{array}{ccccccccccccccc}
 & & & & & K_{3,0} & K_{0,3} & K_{0,0} & K_{0,2} & K_{2,0} & & & & & \\
\cdots & 1 & 0 & 0 & 0 & 1 & 1 & 1 & 1 & 1 & 0 & 0 & 1 & \cdots \\
 & & & & & K_{3,0} & K_{0,5} & K_{2,0} & & & & & & & \\
\cdots & 1 & 0 & 0 & 0 & 1 & 1 & 1 & 0 & 0 & 1 & \cdots & & & \\
 & & & & & K_{3,2} & K_{2,3} & & & & & & & & \\
\cdots & 1 & 0 & 0 & 0 & 1 & 1 & 0 & 0 & 1 & \cdots & & & & \\
 & & & & & K_5^* & & & & & & & & & \\
\cdots & 1 & 0 & 0 & 0 & 1 & 0 & 0 & 1 & \cdots & & & & &
\end{array}$$

B. Crack arrestor pairs

Under LLS [41], when all surviving fibers have the same strength, the strength of a bundle observed under an increasing applied load x is determined by the *largest* load concentration factor initially found in the bundle. Failure of a fiber always results in an even higher load on its survivors, thus forcing catastrophic collapse. There can be no damage evolution under increasing load in the form of stable increases in the number of fiber fractures. Under TLS, however, for some configurations and loads x, the most overloaded fibers can fail without the bundle failing. This occurs because the largest load concentration factor K in the resulting configuration

is such that $Kx<1$, and the bundle is stable. For example, for $\theta=2/3$ and $x\geqslant 1/K^*_{i+j}$, the configuration

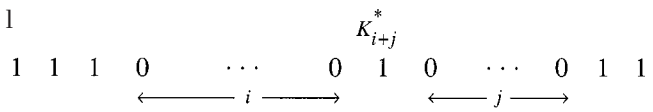

changes upon failure of the isolated fiber to

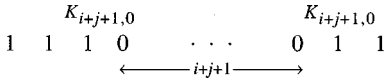

and if $1/K^*_{i+j}\leqslant x<1/K_{i+j+1,0}$ this configuration will be stable, but if $x>1/K_{i+j+1,0}$ this configuration will result in failure. On the other hand, for the configuration

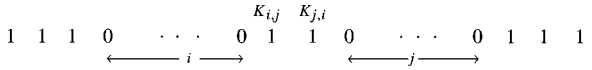

where $i\geqslant j$, failure of the fiber under $K_{i,j}$ will thereafter produce load concentration factors in all subsequent configurations of at least $K_{i,j}$ in magnitude so that the bundle will collapse instantaneously. This was the idea behind Fig. 2. Also if $j=0$, failures under $K_{i,0}$ will always lead to higher load concentration factors. Consequently, we think of a pair of adjacent survivors, ''1 1,'' as a *crack arrestor pair*. Once a fiber in the pair fails, the bundle collapses catastrophically. For a given load x, to determine the bundle strength we must be careful to consider those configurations where failure is not only initiated but sustained to catastrophic failure under the TLS rule. The previous examples have demonstrated that it is those configurations where the largest load concentration factor is of the type K^*_j of Eq. (11b) that require careful study.

Three other points should be made: First, TLS is monotone; that is, the load concentration factor on any given survivor does not decrease by the failure of other fibers. Second, all fibers loaded beyond their strength at any stage fail instantly; that is, we need not be concerned with the order of failures. Third, a fiber subadjacent to broken fibers can never be the most heavily overloaded fiber since $K_{i,j}\geqslant K_{j,i}$ for $i\geqslant j$.

C. Load partitioning for $\theta=2/3$

Unless otherwise stated, we assume henceforth that $\theta=2/3$ in the TLS rule since the contrast with LLS is the most striking. In this case, Eqs. (11a) and (11b) indicate that the various load concentration factors associated with broken fibers have possible values $1+k/6$ for $k=1,2,3,\ldots$. For $k\geqslant 2$, all values of k are connected with certain values of K^*_i and $K_{i,j}$, which are the largest load concentration factors in certain configurations. In particular $K^*_i=1+3i/6$ for $i=2,3,4,5,\ldots$, which corresponds to $k=6,9,12,15,\ldots$. Also $K_{i,0}=1+2i/6$ for $i=1,2,3,4,\ldots$, which corresponds to $k=2,4,6,8,\ldots$, and $K_{i,1}=1+(2i+1)/6$ for $i=1,2,3,4,\ldots$, which corresponds to $k=3,5,7,\ldots$. Note that $K_{i,0}=K_{i-1,2}=K_{i-2,4}=\cdots$, and $K_{i,1}=K_{i-1,3}=K_{i-2,5}=\cdots$, where our interest is in all cases where the second subscript is less than or equal to the first.

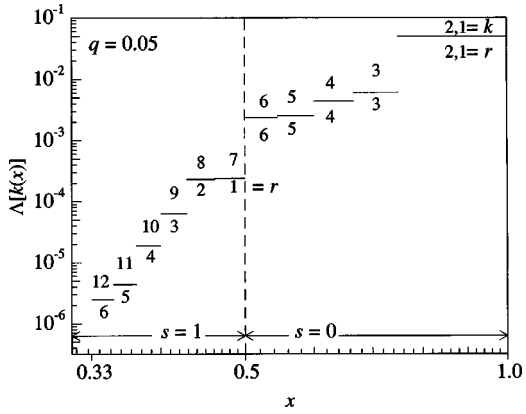

FIG. 5. Plot of $\Lambda[k(x)]$ versus x for $q=0.05$ and $s=0,1$, and $r=1,2,\ldots,6$, and where $k=6s+r$ where the dependence of k, r and s on x is given by Eq. (15). The probability of failure of a bundle of n fibers is $G_n(x)\approx 1-\exp\{-n\Lambda[k(x)]\}$.

For a bundle of n fibers, we let the random variable X_n denote its strength (the smallest load under which the bundle fails), and we let $G_n(x)$, $x\geqslant 0$ be its distribution function. Since the strength of an intact fiber is 1, the strength of a bundle must be a load x satisfying $Kx=1$, where $K=1+k/6$ for some non-negative integer k. Note that K is associated with an unfailed fiber within some local fiber break configuration occurring as the bundle fails, and which becomes catastrophically unstable once that fiber fails. Thus X_n has the possible outcomes

$$x_k=\frac{6}{6+k},\quad k=0,1,2,3,4,5,\ldots, \tag{12}$$

with the exception of $x_1=6/7$ which cannot occur under TLS with $\theta=2/3$. Thus $G_n(x)$ is a discrete distribution. Note in particular that if all fibers in the bundle are intact, then $x_k=1$ and thus, $G_n(x)=1$, $1\leqslant x<\infty$.

For a given load $0<x<1$, to determine the probabilities for failure of a bundle it is useful to consider two ways of partitioning the failure load range $0<x<1$ into coarse and fine partitions as illustrated in Fig. 5. The coarse partition is described in terms of *load spans*, and is given by

$$\frac{1}{1+s+1}\leqslant x<\frac{1}{1+s},\quad s=0,1,2,3,\ldots. \tag{13}$$

The fine partition is described in terms of *load regions* and is given by

$$\frac{6}{6+k}\leqslant x<\frac{6}{6+k-1},\quad k=1,2,3,\ldots. \tag{14a}$$

Note that for a load x in load region k, the bundle fails if $X_n\leqslant 6/(6+k)$ but survives if $X_n\geqslant 6/(6+k-1)$. Note also that the sth load span is the union of load regions $k=6s+1,6s+2,\ldots,6s+6$. To study certain similarities that oc-

cur in failure configurations in different load spans it is useful to divide each load span into six *subspans*, which actually correspond to load regions. Specifically, the kth load region may be written $k=6s+r$ for some subspan r in span s where $r=1,2,\ldots,6$. Thus Eq. (14a) can be written as

$$\frac{6}{6+6s+r}\leqslant x<\frac{6}{6+6s+r-1},$$

$$r=1,2,3,\ldots 6, \text{ and } s=1,2,3,\ldots . \tag{14b}$$

The following relationships can be seen by inspection of Eqs. (13) and (14):

$$s=\lceil(1-x)/x\rfloor-1=\lceil 1/x\rfloor-1, \tag{15a}$$

$$k=\lceil 6(1-x)/x\rfloor=\lceil 6/x\rfloor-6+1, \tag{15b}$$

and

$$r=\lceil 6/x\rfloor-6\lceil 1/x\rfloor+1=k-6s, \tag{15c}$$

where ''$\lceil\ \rfloor$'' denotes the integer part of a real number except when the number is an integer, in which case, we take the next smallest integer.

The partitioning scheme we have devised allows us to characterize all possible failure configurations for a bundle under load $0<x\leqslant 1$ in terms of their local structure of ''0''s and ''1''s, and to assess their probabilities of occurrence. This task is considered next and is tedious. Much of the complication arises from the fact that the structure of the configurations differs in adjacent load regions in Eq. (14a). However, for fixed r in Eq. (14b) this structure turns out to be similar for different s, so there is a quasiperiodicity in s.

IV. FAILURE CONFIGURATIONS AND PROBABILITIES FOR SMALL s

We now study how to identify a local fiber configuration that will result in failure of a bundle under a given load x. The idea is that bundle failure will occur if and only if at least one such configuration occurs somewhere in the bundle, and there will be some position in the bundle working from left to right, where such a failure configuration first appears. With the exception of very small bundles, such configurations will involve the breakdown of a crack arrestor pair defined earlier as a pair of consecutive ones, ''1 1'' with an ''0'' on one or both sides. If one of the fibers in the pair is overloaded, then the pair fails and the whole bundle collapses as all remaining fibers suffer increased loads in succession.

First we consider an arbitrary interior fiber, i, and associate with it a list of irreducible, local failure configurations associated with a given load x. These configurations are described in terms of k and s, which are determined from x by Eqs. (13) and (14). Each failure configuration will have either one or two crack arrestor pairs, and fiber i will be the second fiber in the first (leftmost) crack arrestor pair. When a configuration has only one crack arrestor pair, the configuration will be constructed such that fiber i is the first of the pair to succumb to overloads, which will come from breakdown of the configuration to its right (or both may fail simultaneously). When a configuration has a second crack arrestor pair to the right of the first, the second pair will fail first due to a failure progression that causes failure of the leftmost fiber in that pair (or both may fail simultaneously). In this way we account for crack arrestor pairs failing under overloads coming from the left, or the right. Note that bundles with a crack arrestor pair at fiber i that fails from the left are accounted for in configurations for some other fiber $i'<i$.

For all possible configurations associated with fiber i leading to failure within load region k, we let $P(k)$ be the sum of their probabilities. Note that these configurations represent disjoint events. $P(k)$ will be essential to determining the distribution function $G_n(x)$ for bundle strength, and ignoring boundary effects will be independent of i.

A. Critical load concentrations and initiating clusters

For load region k, whereby $6/(6+k)\leqslant x<6/(6+k-1)$, there are two critical load concentration factors to keep in mind:

$$\mathcal{K}_{i,k}=1+(1/2)\lfloor(k+2)/3\rfloor, \tag{16}$$

the minimal load concentration factor associated with *crack initiation*, and

$$\mathcal{K}_{c,k}=1+k/6, \tag{17}$$

the minimal load concentration factor associated with *catastrophic crack propagation*, where ''$\lfloor\ \rfloor$'' denotes integer value. If a configuration is to fail under load x in load region k, a load of at least $\mathcal{K}_{c,k}x$ must occur on some fiber (typically requiring failure of several fibers after initiation under $\mathcal{K}_{i,k}x$ on a fiber). Clearly $\mathcal{K}_{i,k}\geqslant\mathcal{K}_{c,k}$. Crack initiation in a configuration requires an *initiating cluster* of either I_k contiguous ''0''s, or I_k ''0''s interrupted by at most one ''1,'' where from Eq. (16)

$$I_k=\lfloor(k+2)/3\rfloor=2s+\lfloor(r+2)/3\rfloor. \tag{18}$$

This is most easily seen by writing out cases $k=1,2,3,\ldots$ and observing the patterns. For example, if there is a ''1'' interrupting I_k ''0''s, then it will fail under load $\mathcal{K}_{i,k}x$. An I_k+1 cluster results, which will grow by failing sequentially any isolated ''1''s it encounters on either side, until it encounters a crack arrestor pair. Such a pair, in turn, will fail if and only if at least one of its two fibers comes under a load at least $\mathcal{K}_{c,k}x$, thus causing bundle collapse. Note that the critical load concentration $\mathcal{K}_{c,k}x$ may occur in one or both fibers in a crack arrestor pair.

B. Load span $s=0$

We study first the uppermost load span $1/2\leqslant x<1$ associated with $s=0$, starting with the upper load region, $k=1$ and working on down (see Fig. 5). In general, the number of failure configurations, their lengths and their complexities increases as x decreases. Therefore to gain insight, it is best to study these simple configurations before trying to under-

stand their general structure. As we progress to failure configurations associated with larger k and s, i.e., to smaller applied loads x, we will illustrate the emergence of certain features that are part of the more complex, general structure. As the complexity increases with larger s, it is necessary to impose special conventions, such that these failure configurations are *irreducible*, i.e., as short as possible on the right end, and that no double counting occurs as i varies over the bundle.

Two cases are trivial: For $x \geqslant 1$ all fibers are overloaded and the bundle fails automatically, so its probability of failure is $G_n(x)=1$. The case $3/4 \leqslant x < 1$ (which covers $k=1,2$; $s=0$, $r=1,2$) is also trivial since just one ''0'' in the bundle causes collapse. Thus $G_n(x)=1-(1-q)^n$.

For the case $2/3 \leqslant x < 3/4$ ($k=3$; $s=0$, $r=3$), three nontrivial failure configurations can be constructed. From Eq. (18), $I_3=1$, so the initiating cluster can have no interrupting ''1''s, and from Eqs. (16) and (17), $\mathcal{K}_{i,3}=\mathcal{K}_{c,3}=3/2$, so initiation implies collapse. The configuration list and associated probability sum $P(k=3)$ associated with fiber i in the bundle is

$$\begin{array}{c} \overset{i}{} \\ 1\,1\,1\,0\,0\,\mathrm{Y} \\ 1\,1\,1\,0\,1\,0 \\ 1\,1\,1\,0\,1\,1\,0 \end{array}$$

$$P(3)=p^3q(q+pq+p^2q)\approx 3q^2, \tag{19}$$

where the rightmost approximation in $P(k)$ assumes small q. Here ''Y'' implies the fiber is either a ''1'' or a ''0'' and hence has probability $p+q=1$. (This designation will be convenient later.) The required crack arrestor pair is designated on the left in all three configurations with the necessary ''0'' to its right. Note that we have specified the fiber furthest to the left as a ''1'' because failure of fiber i must, by convention, be caused from the right. Note, however, that the third configuration has a second crack arrestor pair which fails first and by both ''1''s failing simultaneously.

The case $3/5 \leqslant x < 2/3$ ($k=4$; $s=0$, $r=4$) gives $I_4=2$, $\mathcal{K}_{i,4}=2$ and $\mathcal{K}_{c,4}=5/3$ and has the following nontrivial configuration list and associated probability sum:

$$\begin{array}{c} \overset{i}{} \\ 1\,1\,1\,0\,0\,\mathrm{Y} \\ 1\,1\,1\,0\,1\,0 \\ 1\,0\,1\,1\,0\,0\,\mathrm{Y} \\ 1\,0\,1\,1\,0\,1\,0 \end{array}$$

$$P(4)=p^3q^2(1+q)(1+p)\approx 2q^2. \tag{20}$$

Since initial failure gives rise to a load concentration greater than $\mathcal{K}_{c,4}$, the first break again implies collapse. Here, we see crack initiation at the interrupting ''1'' (2nd and 4th configurations) outside of fiber i. Note that configurations with two crack arrestor pairs are not needed because to fail before the first, the second crack arrestor pair would need to fail from its right. But then the critical segment of this configuration would be a configuration for a later fiber $i'>i$.

The case $6/11 \leqslant x < 3/5$ ($k=5$; $s=0$, $r=5$) gives $I_5=2$, $\mathcal{K}_{i,5}=2$ and $\mathcal{K}_{c,5}=11/6$ and yields configurations and probability sum:

$$\begin{array}{c} \overset{i}{} \\ 1\,1\,1\,0\,0\,0\,\mathrm{Y} \\ 1\,1\,1\,0\,1\,0\,\mathrm{Y} \\ 1\,1\,1\,0\,0\,1\,0 \\ 1\,0\,1\,1\,0\,0\,\mathrm{Y} \\ 1\,0\,1\,1\,0\,1\,0 \\ 1\,1\,1\,0\,0\,1\,1\,0 \end{array}$$

$$P(5)=p^3q^2[1+q(1+p)^2]\approx q^2. \tag{21}$$

The last configuration has two crack arrestor pairs. The second pair is (and must be) flanked by ''0''s, has an initiating cluster ($I_5=2$) to its left, and fails first through failure of its leftmost ''1.'' In the fourth configuration, the first isolated ''0'' is necessary to ''help'' the initiation cluster fail the second fiber of the crack arrestor pair. By convention the string of ''0''s to the left of the first crack arrestor pair must be shorter than I_k to ensure that the failure initiates on the right.

The last case in $s=0$ is $1/2 \leqslant x < 6/11$ ($k=6$, $s=0$, $r=6$), which has $I_6=2$, $\mathcal{K}_{i,6}=2$ and $\mathcal{K}_{c,6}=2$, and the following list and probability sum (using various reductions, such as $p+q=1$):

$$\begin{array}{c} \overset{i}{} \\ 1\,1\,1\,0\,0\,0\,\mathrm{Y} \\ 1\,1\,1\,0\,1\,0\,\mathrm{Y} \\ 1\,1\,1\,0\,0\,1\,0 \\ 1\,0\,1\,1\,0\,0\,0\,\mathrm{Y} \\ 1\,0\,1\,1\,0\,1\,0\,\mathrm{Y} \\ 1\,0\,1\,1\,0\,0\,1\,0 \\ 1\,1\,1\,0\,0\,1\,1\,0\,0 \\ 1\,0\,1\,1\,0\,0\,1\,1\,0\,0 \\ 1\,1\,1\,0\,0\,1\,1\,0\,1\,0 \\ 1\,0\,1\,1\,0\,0\,1\,1\,0\,1\,0 \end{array}$$

$$P(6)=p^3q^2(1+q)[1+pq+q^2(p^2+q^2)]\approx q^2. \tag{22}$$

Interestingly, in some of the above configurations an I_6 initiation cluster (e.g., ''0 0'') by itself may not cause failure. For example, in the last two configurations we see two cases where the second crack arrestor pair fails by overloading both its fibers in a ''tie.'' Note also that removing all fibers to the left of fiber i in both configurations leaves ''1 0 0 1 1 0 1 0,'' which might seem to be a possible failure configuration for fiber $i'=i+4$. But the crack arrestor pair has an I_6 to its left so both fibers will fail in a tie, thus violating our convention. In this way double counting is avoided.

We still must consider boundary effects as follows: For fibers $1 \leqslant i \leqslant I_k+2$ near the left boundary, some or all configurations in the list must be truncated on the left, and only

those that still cause failure of fiber i (assuming the truncated fibers transmit no load) must remain in the list. Truncation is also possible at the right end of the bundle by a similar rule. By this scheme some load is lost at the edges, but the effects turn out to be negligible as n grows large.

Regarding the above constructions there are several important points to be made: First our failure configurations must be constructed carefully to take advantage of the Chen-Stein method of Poisson approximation to tightly estimate $G_n(x)$. (See Appendix B.) It may be tempting to delete the left-most ''1'' in each configuration, but it turns out that the resulting estimate of $G_n(x)$ would be too inaccurate, that is, in using the Chen-Stein theorem, the error bounds would be of the order of $G_n(x)$ and thus, would be too loose. This occurs because without the leftmost ''1,'' configurations in the respective lists of two fibers, i and i', which are close to each other, would share too many common fibers. On the one hand, we must construct configurations for fiber i that overlap minimally those for a neighboring fiber i', but, on the other hand, we must be careful that no possible failure configuration is neglected. Second, for configurations that have two crack arrestor pairs, as occurs for $k=5$ and 6, the fiber sequence between them must contain an initiating cluster. Third, the failure configurations we construct must be irreducible.

The local failure configurations listed for fiber i may not seem at first to exhaust all local possibilities. However, those that are omitted will have structure *implying* the occurrence of a failure configuration in the list of some other fiber $i' < i$ to the left (including the special boundary lists); that is they will actually be redundant extensions of these earlier configurations, which would already have failed the bundle. For example, consider the configuration ''1 0 0 1 1 0 0 1 0'' for $k=6$, which is not in our list, but which clearly causes failure of fiber i (the 2nd fiber in the crack arrestor pair). This configuration violates the convention that the string of 0's to the left of fiber i must be less than I_k. To explain, we note that this configuration can be reduced to ''1 0 0 1 1 0 0'' and still cause failure. Now to its left must be a ''1,'' or ''1 0'' or ''1 0 0'' or ''1 0 0 0'' and so on. If it is a ''1,'' then to the left of that must be another ''1,'' or ''1 0'' or ''1 0 0'' or ''1 0 0 0'' and so on again. If the latter is a ''1,'' we have ''1 1 1 0 0 1 1 0 0'' which is in the list of fiber $i'=i-4$, and the same is true if the latter is a ''1 0.'' On the other hand, if we add ''1 0'' to the reduced configuration, we obtain ''1 0 1 0 0 1 1 0 0'' which can be reduced further to ''1 0 1 0 0.'' We can then add to the left of this configuration and so on, so that eventually (with reductions along the way) we arrive at a failure configuration for some fiber i', possibly near the left boundary. For example ''1 0 0 1 1 0 0'' is a boundary configuration for $i=1$.

C. Load span $s=1$

We now turn to the load span, $s=1$, wherein $1/3 \leqslant x < 1/2$, and present only a few cases for illustration. The case $6/13 \leqslant x < 1/2$ ($k=7$, $s=1$, $r=1$) gives $I_7=3$, $\mathcal{K}_{i,7}=5/2$ and $\mathcal{K}_{c,7}=13/6$ and has the failure configuration list and probability $P(k)$:

$$
\begin{array}{l}
\overset{i}{1\,1\,1\,0\,0\,0\,0\,Y} \\
1\,1\,1\,0\,0\,0\,1\,0 \\
1\,1\,1\,0\,1\,0\,0\,Y \\
1\,1\,1\,0\,0\,1\,0\,Y \\
1\,1\,1\,0\,1\,0\,1\,0\,0\,\dagger \\
1\,1\,1\,0\,1\,0\,1\,0\,1\,0\,0 \\
1\,1\,1\,0\,1\,0\,1\,0\,1\,0\,1\,0\,0 \\
\qquad \vdots \\
\qquad \text{(continue introducing '01' pairs)} \\
\qquad \vdots \\
1\,0\,1\,1\,0\,0\,0\,Y \\
1\,0\,1\,1\,0\,1\,0\,0\,Y \\
1\,0\,1\,1\,0\,0\,1\,0\,Y \\
1\,0\,1\,1\,0\,1\,0\,1\,0\,0 \\
\qquad \vdots \\
\qquad \text{(endings continuing as above beginning with '†')} \\
\qquad \vdots \\
1\,0\,0\,1\,1\,0\,0\,0\,0\,Y \\
\qquad \vdots \\
\qquad \text{(same endings as just listed)} \\
\qquad \vdots \\
1\,1\,1\,0\,0\,0\,1\,1\,0
\end{array}
$$

$$
\begin{aligned}
P(7) &= p^3q^3(1+q+q^2)[1+p+p/(1-pq)]-p^3q^3(p^3) \\
&\approx 2q^3. \qquad (23)
\end{aligned}
$$

We now see the emergence of unbounded sequences in number and length to the right of the first crack arrestor pair. Such configurations have initiating clusters only at the very right end, which can be far from the crack arrestor pair. Configurations here with two crack arrestor pairs cannot be constructed to have ''1 0 0'' at the left end, since they could then be reduced to ones with one pair.

The case $3/7 \leqslant x < 6/13$ ($k=8$, $s=1$, $r=2$) gives $I_8=3$, $\mathcal{K}_{i,8}=5/2$ and $\mathcal{K}_{c,8}=7/3$, and is similar to $k=7$ except ''1 0 1 1 0 0 0 Y'' is replaced by ''1 0 1 1 0 0 0 0 Y'' and ''1 0 1 1 0 0 0 1 0 Y.'' Also the last configuration is replaced by

$$
\begin{array}{l}
1\,1\,1\,0\,0\,0\,1\,1\,0\,0 \\
1\,1\,1\,0\,0\,0\,1\,1\,0\,1\,0\,0 \\
1\,1\,1\,0\,0\,0\,1\,1\,0\,1\,0\,1\,0\,0 \\
\qquad \vdots \\
\qquad \vdots \\
\qquad \vdots
\end{array}
$$

as well as these same ones but with ''1 0'' replacing ''1'' at the left end. Unlike all previous cases, the configurations with two crack arrestor pairs can be unbounded in number and length. We find

$$P(8)=p^3q^3(1+q)[q+pq+p+p/(1-pq)]$$
$$+p^3q^3(q^2)[1+p+p/(1-pq)]$$
$$+p^3q^3(1+q)[p^2q^2+p^3q^3/(1-pq)]$$
$$\approx 2q^3. \tag{24}$$

For $k=9$ the configurations are longer, but the structure is basically the same as for $k=8$. For $k=10$, however, more complex right endings of the type ''1 0 1 0 0 0'' and ''1 0 0 1 0 0'' emerge, which come from longer initiating clusters ($I_{10}=4$) occurring only at the far right. For $k=11$, arrangements of fibers between the crack arrestor pairs can be longer thus permitting initiation clusters with interrupting ''1''s (for example ''1 1 1 0 1 0 0 0 1 1 0''). The same is true for $k=12$. For even larger k this feature becomes more prominent as the distance between crack arrestor pairs increases further to make more room for large I_k. Generally, I_k will be about $2s$ in length, whereas up to about $3s$ fibers are possible between crack arrestor pairs. For small q, we find that $P(9)\approx 10q^4$, $P(10)\approx 3q^4$, $P(11)\approx 14q^5$, and $P(12)\approx 8q^5$. Interestingly, this simple structure in integer powers of q, will not prevail for larger s, as quantities related to eigenvalues of certain recursions begin to emerge.

As a final comment, we see already the probability of failure of a bundle at load $x=1/3$ [at the bottom end of load region $k=12$ by Eq. (13)], is becoming rather small, making Monte Carlo simulation problematic. To explain, we take for example $q=1/10$ where we find $P(12)\approx 0.00008$. Thus bundles would need to have about $n=12\,500$ fibers to have roughly an equal chance of failing or not failing. On the other hand, the configurations that cause failure are still not long enough to reveal subtle probability features emerging from eigenvalue analysis, which ultimately determine the character of the distribution for strength and the size effect.

V. GENERAL FAILURE CONFIGURATIONS

In this section, we describe the system of failure configurations needed for failure of a bundle of n fibers under loads $0<x<1/2$ ($s\geqslant 1$). Recall that upon fixing $s\geqslant 1$ and $1\leqslant r\leqslant 6$, we are equivalently fixing $k=6s+r$ and the load region,

$$\frac{6}{6+k}\leqslant x<\frac{6}{6+k-1}. \tag{25}$$

Given this load region, we construct sets of configurations of ''1''s and ''0''s such that the bundle fails if and only if at least one of them occurs somewhere in the bundle, and the Chen-Stein method for Poisson approximation gives a sufficiently tight bound (Appendix B), which roughly means that they should be sufficiently distinct in structure. We will present their general structure and sizes in terms of s and r. As before we associate with these configurations some fiber i in the bundle, which is again the second fiber in the leftmost crack arrestor pair ''1 1'' in the configuration that also has an ''0'' immediately to its right.

Before beginning, we caution that while the basic ideas motivated in Sec. IV may be straightforward to grasp, fully appreciating the detailed structure of the configurations that arise is difficult and tedious, and requires one to write out and study the various cases. Much of the complication and tedium occurs because, for any given s, the configurations needed for failure change subtly when r varies over 1 to 6. This occurs because the load redistribution involves units of 1/6 to subadjacent fibers but 1/3 to adjacent fibers, as was seen in Sec. IV. Ideally we would write out below the cases $r=1,2,\ldots,6$ in succession but this is not practical due to space limitations. Thus we have devised the following compact description of the structure of the various failure sequences for each load x.

To begin, we consider cases where fiber i is an *interior* fiber of the bundle such that boundary effects can be ignored. An interior fiber is at least $2s+3$ fibers from the left boundary and about $5s+6$ fibers from the right boundary.

A. Type I configurations

The first failure configurations of interest are called type I configurations, and contain only one crack arrestor pair. The simplest set contains configurations with the structure

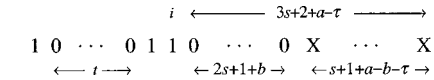

where X...X is a sequence of ''0''s and ''1''s such that no two ''1''s are adjacent. Also, from Eq. (15) the key integers used in defining the string lengths in these configurations are

$$a=a(r)=\lfloor (r-1)/2\rfloor,\quad b=b(r)=\lfloor (r-1)/3\rfloor,$$
$$\tau=\tau(r)=\lfloor (r+t)/2\rfloor-\lfloor r/2\rfloor, \tag{26a}$$

where ''$\lfloor\ \rfloor$'' means integer value. Thus $0\leqslant a\leqslant 2$ and $0\leqslant b\leqslant 1$, and as before our convention dictates that $0\leqslant t\leqslant 2s+b<2s+b+1=I_k$, which is the initiating cluster length defined by Eq. (18). It can be seen that $0\leqslant\tau\leqslant\lfloor s+(r+b)/2\rfloor-\lfloor r/2\rfloor$ and $0\leqslant\tau\leqslant s+1+a-b$. To relate t to τ, we define

$$c=\begin{cases}0 & r=2,4,6,\\ 1 & r=1,3,5,\end{cases} \tag{26b}$$

so that by Eq. (26a) $t=0$ for $\tau=0$, but $t=2\tau-c$, $2\tau-c+1$ for $\tau\geqslant 1$. Note that the first fibers to fail are the ''1''s in X···X starting from the left, followed by the crack arrestor pair beginning with fiber i.

Another set of type I configurations is similar to the first except that each has an isolated ''1'' introduced into the $2s+b+1$ cluster and thus has the structure

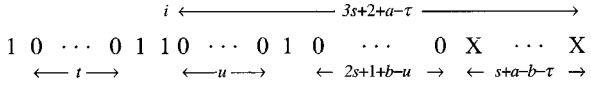

where $1\leqslant u\leqslant 2s+b$ and $0\leqslant\tau\leqslant s+a-b$. Here the first fiber to fail is the isolated ''1'' in the initiating cluster, followed by the ''1''s in X···X starting from the left followed by the crack arrestor pair beginning with fiber i.

The most important set of type I configurations contains configurations of the form

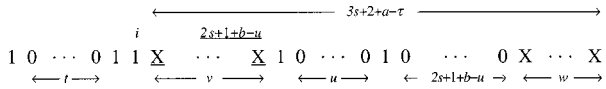

where the subsequence $\underline{X}\cdots\underline{X}$ is the same as X···X, except that the terminal element on each end must be an ''0'' and where ''$\underline{d}$'' above an end of a subsequence means that the number of contiguous ''0''s at this end must be less than d. In the above, $1\leqslant u\leqslant 2s+b-1$, $1\leqslant v\leqslant s-1+a-b-\tau$, $w=s-1+a-b-\tau-v$, and $0\leqslant w\leqslant s+a-b-\tau-2$. Here the failure progression begins with the isolated ''1'' in the initiating cluster, followed by the ''1''s in X···X starting from the left, followed by the ''1''s in $\underline{X}\cdots\underline{X}$ starting from the right, followed by the crack arrestor pair beginning with fiber i. It turns out that the three sets of configurations just described are the *dominant* configurations of type I in determining the probability of bundle failure.

There is one more set of type I configurations, which has long configurations structured as

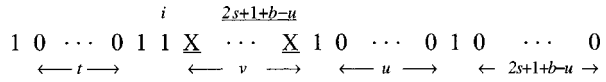

where $s+a-b-\tau\leqslant v\leqslant\infty$. It turns out that these become negligible in importance for large k, that is, they contribute negligibly to the probability of failure of large bundles at lower loads x. Thus we label these as type I′ configurations.

B. Type II configurations

The second type of failure configurations of interest are called type II configurations, which contain two crack arrestor pairs. The simplest of these have the structure

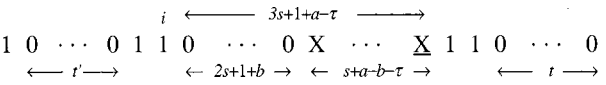

where $1\leqslant\tau\leqslant s+a-b$, and $t=2\tau-c$, and where $0\leqslant t'\leqslant t-1$. Here the subsequence X···X is the same as X···X, except that the terminal element on the right must be a ''0.'' Note that failure proceeds with failure of the ''1''s in X···X beginning from the left followed by the *second* crack arrestor pair starting with its first ''1,'' which requires the help of loads from the rightmost string of ''0''s. Only then does the first crack arrestor pair fail starting with fiber i, which requires the help of loads shifted from the leftmost string of ''0''s. Another set of type II configurations is constructed by inserting an isolated ''1'' into the $2s+b+1$ initiation cluster to get

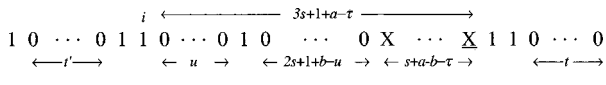

where $1\leqslant\tau\leqslant s+a-b-1$, $0\leqslant t'\leqslant t-1$ and $t=2\tau-c$. Here the failure progression is as just described except that the isolated ''1'' in the initiating cluster fails first. Notably these only occur for $s\geqslant 3$, that is, $x<1/4$.

The most important configurations of type II, are

where $1\leqslant\tau\leqslant s+a-b-3$, $0\leqslant t'\leqslant t-1$, $t=2\tau-c$, $1\leqslant u\leqslant 2s-1+b$, $1\leqslant v\leqslant s-2+a-b-\tau$, and $0\leqslant w\leqslant s+a-b-\tau-3$, and where $w=s+a-b-t-v-2$. Here failure proceeds with failure of the isolated ''1'' in the initiating cluster, followed by the ''1''s in X···X and $\underline{X}\cdots\underline{X}$ spreading out from the initiating cluster, and then by the *second* crack arrestor pair starting with its first ''1,'' which requires the help of loads from the rightmost string of ''0''s. Only then does the first crack arrestor pair fail starting with fiber i, and this requires the help of loads shifted from the leftmost string of ''0''s. These configurations only occur for $s\geqslant 3$ and dominate as s grows large.

All of the type II configurations can be taken as dominant, in that we will sum over them all in determining the dominant terms in the probability of bundle failure for large k.

C. Type III configurations

We also have type III configurations, which are constructed by modifying type II configurations at their right ends as follows: The simplest modification involves replacing the t contiguous ''0''s at the right end by

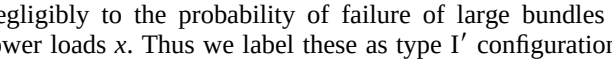

where $1\leqslant u'\leqslant t-1$ and automatically $1\leqslant u'\leqslant 2s+b$. We modify only those configurations of type II where immediately to the left of the second crack arrestor pair, ''1 1,'' there are fewer than $2(s+a-b)-c$ contiguous ''0''s. Otherwise we would create configurations with type I configurations as part of them (for some later fiber i'). A more complex modification of type II configurations involves replacing the t contiguous ''0''s at the right end by

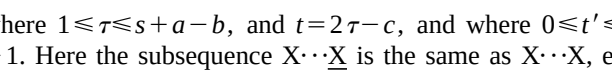

where now $1\leqslant u'\leqslant 2s+b-1$ and $1\leqslant v'\leqslant s+a-b-3$. We modify only those that have fewer than $2(s+a-b-2-v')-c$ contiguous ''0''s immediately to the left of the second ''1 1'' pair.

The last modification covers the case where there are at least $2(s+a-b-2-v')-c$ contiguous ''0''s immediately to the left of the second ''1 1'' pair, in which case $1\leqslant v'<\infty$ (i.e., until we run out of fibers in the bundle but still have failure). Type III configurations are not dominant, as they will be seen to be negligible in probability as k increases.

Note that any other failure configuration we attempt to construct will in whole or in part coincide with a failure configuration associated with some other fiber i'. Though the system described here for constructing failure configurations is not the only one possible, all properly selected systems (structured to be sufficiently distinct and to avoid double counting) will give the same asymptotic results up to

the same order of error in the approximation. (See Harlow and Phoenix [41] for two distinct constructions in the case of local load-sharing, one being more complex than the other and leading to a reduction in the error of approximation for very large k.)

D. Boundary effects

Finally, we need to account for boundary effects. When the intact fiber i lies between $2<i\leqslant 2s+b+2$ near the left boundary, we associate with fiber i the part of the failure configuration to the right of its first ''0.'' This first ''0'' must be positioned no lower than the first fiber in the bundle, and the first ''1'' is deleted if it lands at the fiber zero position (where there really is no fiber). For $i=1,2$ we consider only those configuration patterns beginning with ''1 1 1,'' i.e., $t',t=0$, then delete the ''1''s to the left of the first fiber in the bundle: non existent fibers -1 and 0 for fiber $i=1$ and fiber 0 for $i=2$. Finally we add to the list of configurations for fiber 1, all configurations that begin with ''1 1 1 0'' where the ''0'' is positioned at fiber 1, and then we delete the ''1 1 1''s on the left from each. For fiber i near the right end of the bundle, we truncate all configurations extending past the right end and then keep only those causing failure. Note that for $i>n-2s-1-b$ the list for fiber i has no failure configurations. Note also that every fiber of the bundle will have configurations in its list that must be truncated at the right, but for $i<n-4s$, the truncation will involve negligible configurations. At the left end for $2s<i$ the truncations will also be negligible. In conclusion, the total number of fibers with configurations significantly influenced by the boundary is of order $6s$, which will become negligible for large n.

VI. PROBABILITIES FOR CONFIGURATIONS FOR MODERATE s

We now evaluate and sum the probabilities for types I, II, and III configurations associated with a given interior fiber i as presented in Sec. V. These will apply to moderate values of s. First we need to define several key quantities that arise in the summations. We note that carrying out these summations to yield the quantities given below is very tedious and once more we have omitted details in the interest of brevity.

A. Important quantities arising in failure configuration probabilities

One key quantity is the function $\Phi(s)$, which is

$$\Phi(s)=q^{2s+1}\delta^s p^5\left(\frac{\delta}{\delta+2p}\right)^2\left(\frac{\delta}{q^2}\right), \tag{27}$$

where δ is the largest root of the characteristic equation $\delta^2-q\delta+qp=0$ (Appendix A). We also let

$$\beta_j(s,r)=\left(\frac{\delta+2p}{p}\right)\left\{\frac{\delta}{p}+(2s+b)+I(j)(2s+b-1)\times\left[\frac{q^2p}{\delta^{4-j}(1-\delta)}\right]\right\},\quad j=0,1,2,3, \tag{28}$$

where $I(j)$ is an indicator function defined by $I(j)=0$, when $j=0$ and $I(j)=1$, when $j=1,2,3$, and we recall $b=b(r)=\lfloor(r-1)/3\rfloor$. Two additional quantities of interest are

$$\Omega_1(s,r)=(1+q)\sum_{i=0}^{s+a-b-2}\left(\frac{q^2}{\delta}\right)^i(s+a-b-2-i) \tag{29}$$

and

$$\Omega_2(s,r)=(1+q)\left[\frac{1-(q^2/\delta)^{s+a-b-1}}{1-(q^2/\delta)}\right], \tag{30}$$

where we recall $a=a(r)=\lfloor(r-1)/2\rfloor$. Also we have the quantity

$$\xi(s,r)=\left(\frac{q^2}{\delta}\right)^{s+h}\left[(1+q)\left(\frac{\delta}{q^2}\right)^{1-g}\beta_2(s,r)+(1-g)(1+q)^f\beta_3(s,r)\right], \tag{31}$$

where $f=f(r)=1$, when $r=1,4$, and $f(r)=0$, when $r=2,3,5,6$, and where $g=g(r)=1$, when $r=3,6$, and $g(r)=0$, when $r=1,2,4,5$. Also $h=h(r)=\min\{b(r),c(r)\}$, where $c(r)=1$, when $r=1,3,5$ and $c(r)=0$, when $r=2,4,6$. A sum that arises is

$$\alpha_i=1+q+\cdots+q^i=\left(\frac{1-q^{i+1}}{1-q}\right),\quad i=1,2,3,\ldots, \tag{32}$$

which is used in the following three functions:

$$\zeta(s,r)=(\delta+2p)^2\left(\frac{1}{q^3p^2}\right)\left(\frac{q^2}{\delta}\right)^{s+b}\times\left\{\alpha_{2(s+a-b)-c-5}\left[1+\frac{p}{q}(2s+b+1)\right]+\alpha_{2(s+a-b)-c-3}q\left[1+\frac{p}{q}(2s+b)\right]+\alpha_{2(s+a-b)-c-1}q^2\right\}, \tag{33}$$

$$\omega_1(s,r)=\sum_{i=0}^{s+b-4}(s+b-3-j)\left(\frac{q^2}{\delta}\right)^i\alpha_{2i+1-c}, \tag{34a}$$

and

$$\omega_2(s,r)=\sum_{i=0}^{s+b-4}\left(\frac{q^2}{\delta}\right)^i\alpha_{2i+1-c}. \tag{34b}$$

B. Probability sums for configurations of types I, II, and III

For a given $k=6s+r$ and interior fiber i we let $P_1(k)$ and $P_2(k)$ be the probability of occurrence of a configuration of type I or type II, respectively, as described in Sec. V. (We include configurations of type I′ with those of type I, although the former die out in importance as k increases.) These become the dominating configurations in determining the probability of bundle failure. Calculating these probabili-

ties is tedious and requires summing the probabilities for all configurations of the corresponding types in Sec. V and using results in Appendix A. We let

$$P(k)=P_1(k)+P_2(k), \tag{35}$$

and from the summations find that

$$P_1(k)=\Phi(s)q^{b-c}\delta^{a-b}\{(2s+b-1)[\Omega_1(s,r) - c(s+a-b-2)]+\beta_1(s,r)[\Omega_2(s,r)-c] + \xi(s,r)\} \tag{36}$$

and

$$P_2(k)=\Phi(s)q^{b-c}\delta^{a-b}[(2s+b-1)\omega_1(s,r) + \beta_0(s,r)\omega_2(s,r)+\zeta(s,r)]\left(\frac{q^3p^2}{\delta^3}\right). \tag{37}$$

We also let $P_3(k)$ be the probability for the occurrence of a type III configuration at fiber location i. It can be seen that type III configurations are not dominant because they have two initiating clusters, so that

$$P_3(k)<(2s+1+b)^2(s+a)q^{4s+2+2b}. \tag{38}$$

Note that because of the two initiating clusters, the power in q is doubled as compared to $\Phi(s)$. Thus, as s increases, $P_3(k)$ becomes negligible in magnitude compared to $P(k)=P_1(k)+P_2(k)$. In fact the ratio goes as $O(sq^{2s})$ which decreases dramatically in s for smaller q.

VII. ASYMPTOTIC FORMS OF PROBABILITIES FOR LARGE s

The expressions presented in Sec. VI can be simplified for large s, corresponding to small x, as seen by Eq. (15a). In particular Eq. (28) reduces to

$$\beta_j(s,r)=2s\left(\frac{\delta+2p}{p}\right)\left[1+I(j)\,\frac{q^2p}{\delta^{4-j}(1-\delta)}\right][1+O(1/s)], \quad \text{for } j=1,2,3, \tag{39}$$

where $O(x)/x\to$const as $x\to 0$, and Eqs. (29) and (30) reduce to

$$\Omega_j(s,r)=s^{2-j}(1+q)\left(\frac{\delta}{\delta-q^2}\right)[1+O(1/s)], \quad j=1,2. \tag{40}$$

An important factor in Eq. (40) is

$$\Omega=(1+q)\left(\frac{\delta}{\delta-q^2}\right). \tag{41}$$

In Eq. (34b), we can evaluate the sum to determine

$$\sum_{j=0}^{\infty}\left(\frac{q^2}{\delta}\right)^j\alpha_{2j+1-c} = \sum_{j=0}^{\infty}\left(\frac{q^2}{\delta}\right)^j\left(\frac{1-q^{2j+2-c}}{1-q}\right) = \frac{1}{p}\left[\sum_{j=0}^{\infty}\left(\frac{q^2}{\delta}\right)^j-q^{2-c}\sum_{j=0}^{\infty}\left(\frac{q^4}{\delta}\right)^j\right] = \frac{1}{p}\left(\frac{\delta}{\delta-q^2}-\frac{q^{2-c}\delta}{\delta-q^4}\right), \tag{42}$$

and Eq. (34a) can be treated similarly so that

$$\omega_j(s,r)=\frac{s^{2-j}}{p}\left(\frac{\delta}{\delta-q^2}-\frac{q^{2-c}\delta}{\delta-q^4}\right)+O[s^{2-j}(q^2/\delta)^s], \quad j=1,2. \tag{43}$$

An important factor in Eq. (43) is

$$\omega(c)=\frac{\delta}{p}\left(\frac{1}{\delta-q^2}-\frac{q^{2-c}}{\delta-q^4}\right), \quad c=0,1. \tag{44}$$

Evaluation of the order of Eqs. (31) and (33) yields

$$\xi(s,r)=O[s^2(q^2/\delta)^s] \tag{45}$$

and

$$\zeta(s,r)=O[s^2(q^2/\delta)^s]. \tag{46}$$

Thus the probabilities $P_1(k)$ of Eq. (36) and $P_2(k)$ of Eq. (37) simplify to

$$P_1(k)=2s^2\Phi(s)q^{b-c}\delta^{a-b}(\Omega-c)[1+O(1/s)] \tag{47}$$

and

$$P_2(k)=2s^2\Phi(s)q^{b-c}\delta^{a-b}\left(\frac{q^3p^2}{\delta^3}\right)\omega(c)[1+O(1/s)], \tag{48}$$

where we recall that $k=6s+r$. Thus for large s, $P(k)$ of Eq. (35) becomes

$$P(k)=2s^2\Phi(s)q^{b-c}\delta^{a-b}\times\left[\Omega-c+\left(\frac{q^3p^2}{\delta^3}\right)\omega(c)\right][1+O(1/s)] =2s^2\Phi(s)\Theta(r)[1+O(1/s)], \tag{49}$$

where

$$\Theta(r)=q^b\delta^{a-b}\left[\frac{\delta+q\delta^{1-c}}{\delta-q^2}+\left(\frac{q^2p}{\delta^2}\right)\left(\frac{1}{\delta-q^2}-\frac{q^{2-c}}{\delta-q^4}\right)\right]. \tag{50}$$

The key factor in Eq. (49) is called $\Lambda(k)$, and it is defined as

$$\Lambda(k)=2s^2\Phi(s)\Theta(r). \tag{51}$$

Note that $\Lambda(k)$ reflects the large s behavior of $P(k)$, and thus the probability that a failure configuration as constructed in Sec. V is located at fiber i.

For small q (i.e., for bundles initially with very few ''0''s) and for small p (i.e., for bundles initially with very few unbroken fibers or ''1''s), we can simplify $\Phi(s)$ and $\Theta(r)$ in Eq. (51). From Eq. (A3) we get

$$\delta \approx \begin{cases} \sqrt{q}+q/2, & 0<q\ll 1, \\ 1-p^2, & 0<p\ll 1, \end{cases} \tag{52}$$

so substitution into Eqs. (27) and (50), respectively, gives

$$\Phi(s)\approx q^{2s+1}(\sqrt{q})^s\left(\frac{1}{4\sqrt{q}}+\frac{s}{8}\right) \tag{53a}$$

and

$$\Theta(r)\approx q^{(a+b)/2}, \tag{53b}$$

for small q, and

$$\Phi(s)\approx p^5 e^{-(2s-1)p}(1-sp^2) \tag{54a}$$

and

$$\Theta(r)\approx \frac{1}{p}\left[1+\frac{p}{4}(3-2b)\right], \tag{54b}$$

for small p.

VIII. CHEN-STEIN BOUNDS ON STRENGTH DISTRIBUTION

We now work towards determining the structure of an asymptotic approximation for $G_n(x)$ as the bundle size n grows large and the load x becomes small (i.e., s becomes large), paying particular attention to the magnitudes of the errors of approximation. In particular, we desire an approximation where the error divided by $G_n(x)$ (i.e., relative error) goes to zero as x goes to zero provided n is large enough to avoid boundary effects. This will allow us to accurately estimate failure probabilities even when $G_n(x)$ itself is very small. This has been the main stumbling block in treating such problems in the literature.

Let $\hat{Y}_i=\hat{Y}_i(x)$ be a 0–1 indicator random variable for fiber i, indicating whether or not a failure configuration occurs there under load $x>0$, where $1\leqslant i\leqslant n$. Thus the bundle survives if and only if

$$T_n=T_n(x)\equiv\sum_{i=1}^{n}\hat{Y}_i(x)=0. \tag{55}$$

Our goal is to determine the asymptotic behavior of the distribution function for bundle failure,

$$G_n(x)=P\{T_n(x)>0\},\quad x\geqslant 0. \tag{56}$$

It is useful to break $\hat{Y}_i$ into Y_i and E_i corresponding to the dominant configurations (type I and type II) and negligible configurations (type I′ and type III), respectively, as described in Sec. V. Thus we may write

$$\begin{aligned} P\{T_n>j\}&=P\left\{\sum_{i=1}^{n}\hat{Y}_i>j\right\} \\ &=\sum_{v=0}^{j}P\left\{\sum_{i=1}^{n}Y_i>j-v \text{ and } \sum_{i=1}^{n}E_i=v\right\}, \\ &\qquad j=0,1,\ldots,n. \end{aligned} \tag{57}$$

It can be seen that the probability of occurrence for a negligible failure configuration for fiber i (of type I′ or type III) is less than $(1/s)P(k)$ for s sufficiently large. [See the steps leading to Eq. (49) where $k=6s+r$, and also recall Eq. (38) where the key is $s^3q^{4s}/(s^2q^{2s}\delta^s)\to 0$ as $s\to\infty$ since $q<\delta$.] Thus

$$P\left\{\sum_{i=1}^{n}E_i>0\right\}<(n/s)P(k) \tag{58}$$

so that for s sufficiently large (x sufficiently small)

$$\left|P\{T_n>j\}-P\left\{\sum_{i=1}^{n}Y_i>j\right\}\right|<\varepsilon_{E,n}\equiv(n/s)P(k). \tag{59}$$

This is an important fact in showing that T_n and $\Sigma_{i=1}^{n}Y_i$ have approximately the same distribution.

We now focus on the Chen-Stein theorem to establish a key step, namely

$$\left|P\left\{\sum_{i=1}^{n}Y_i>j\right\}-\sum_{v=j+1}^{\infty}\frac{[nP(k)]^v\exp[-nP(k)]}{v}\right|<\varepsilon_n, \tag{60}$$

where $\varepsilon_n<O(ns^3q^{2s+1+b})P(6s+r)$, which becomes negligible as s increases. To use the Chen-Stein theorem (see Appendix B) the most difficult task is to show that

$$b_2=\sum_{i=1}^{n}\sum_{\substack{j\notin J_i\\ j\neq i}}E[Y_iY_j] \tag{61}$$

is negligible compared to $\lambda_n=nP(k)$ as k grows large, where $E[Y_iY_j]=P\{Y_iY_j=1\}$, and where J_i is a suitable neighborhood of fibers around fiber i such that Y_j is independent of Y_i for $j\notin J_i$. The size of this neighborhood is dictated by the furthest distance to the right and left that the various *dominant* failure configurations can extend. Careful inspection of the ranges of the various indices for the various dominant configurations leads to the choice

$$J_i=\{j:|j-i|\leqslant 6s+3+r\}. \tag{62}$$

For $j\notin J_i$ the dominant configurations for j will *not* overlap those for i.

For $Y_iY_j=1$ to occur, a dominant configuration corresponding to fiber i and one corresponding to fiber j must both occur such that either they do not overlap at all, or, they overlap but have the same values (''0'' or ''1'') for each fiber that is common to both. Thus we consider first cases of

overlapping dominant configurations, and note that each failure configuration has at least one crack arrestor pair where the second ''1'' in the first pair is the index fiber i or j.

Consider an interior fiber i and fiber $j \in J_i$ such that $j \neq i$. For fixed i and $j \in J_i$, there are four cases of overlapping configurations to consider: The first is where dominant configurations of type I for fiber i (excluding those of type I′, which are accounted for in Eq. (58)) overlap *later* dominant configurations of type I for fiber j. The probability that such overlapping occurs is

$$\varepsilon_{i,j}(\mathrm{I,I}) = \Sigma_{t_1}\Sigma_{t_2} P\{1\,0\ \overset{i}{\cdots}\ 0\,1\,1\,\mathrm{Z} \quad \cdots \quad \mathrm{Z}\,1\,0\ \overset{j}{\cdots}\ 0\,1\,1\,\mathrm{Z}' \quad \cdots \quad \mathrm{Z}'\}$$
$$\underset{\longleftarrow t_1 \longrightarrow}{} \quad \underset{\leftarrow 3s+2+a-\tau_1-t_2-1 \rightarrow}{} \quad \underset{\longleftarrow t_2 \longrightarrow}{} \quad \underset{\leftarrow 3s+2+a-\tau_2 \rightarrow}{}$$

for $i<j$. Here $\mathrm{Z}\cdots\mathrm{Z}$ is part of a right-end pattern in a type I configuration and $\mathrm{Z}'\cdots\mathrm{Z}'$ is a full right-end pattern of such a configuration. Also Σ_{t_1} and Σ_{t_2} implies summation over all allowable values of t_1 and t_2. The key observation to make is that such an extended configuration must have two crack initiating clusters with at most $s+a$ positions for j for each configuration of i. It can be shown that for s larger than some threshold value s'

$$\varepsilon_{i,j}(\mathrm{I,I}) < P_1(6s+r)[(2s+1+b)(s+a)q^{2s+1+b}], \tag{63}$$

where it is helpful to review the derivation of $P_1(k)$.

The second case we consider is where dominant configurations of type II overlap later dominant configurations of type I, in which case we consider two distinct possibilities, giving the following probabilities:

$$\varepsilon_{i,j}(\mathrm{II,I}) = \Sigma_{t'_1}\Sigma_{\tau_1} P\{1\,0\ \overset{i}{\cdots}\ 0\,1\,1\,\mathrm{Z} \quad \cdots \quad \mathrm{Z}\,1\,1\,0\ \overset{j}{\cdots}\ 0\,1\,1\,\mathrm{Z}' \quad \cdots \quad \mathrm{Z}'\}$$
$$\underset{\longleftarrow t'_1 \longrightarrow}{} \quad \underset{\leftarrow 3s+1+a-\tau_1 \rightarrow}{} \quad \underset{\longleftarrow t_2 \longrightarrow}{} \quad \underset{\leftarrow 3s+2+a-\tau_2 \rightarrow}{}$$

(when t_1, i and j are all given, t_2 becomes fixed) or

$$\varepsilon_{i,j}(\mathrm{II,I}) = \Sigma_{t'_1}\Sigma_{\tau_1}\Sigma_{t_2} P\{1\,0\ \overset{i}{\cdots}\ 0\,1\,1\,\mathrm{Z} \quad \cdots \quad \mathrm{Z}\,1\,0\ \overset{j}{\cdots}\ 0\,1\,1\,\mathrm{Z}' \quad \cdots \quad \mathrm{Z}'\}$$
$$\underset{\longleftarrow t'_1 \longrightarrow}{} \quad \underset{\leftarrow 3s+1+a-\tau_1-t_2-1 \rightarrow}{} \quad \underset{\longleftarrow t_2 \longrightarrow}{} \quad \underset{\leftarrow 3s+2+a-\tau_2 \rightarrow}{}$$

where $\mathrm{Z}\cdots\mathrm{Z}$ is a piece of a middle pattern in a type II configuration and $\mathrm{Z}'\cdots\mathrm{Z}'$ is a possible complete right end pattern in a type I configuration. For a given choice of i and j, it can be seen that one or the other may occur, but not both. In either case we must have two crack initiating clusters, and it can be shown that for s sufficiently large

$$\varepsilon_{i,j}(\mathrm{II,I}) < P_2(6s+r)[(2s+1+b)(s+a)q^{2s+1+b}]. \tag{64}$$

There are two cases that remain, such as type I dominant configurations overlapping later type II configurations and type II configurations overlapping later type II configurations. These are handled similarly so we omit the details. We find that

$$\varepsilon_{i,j}(\mathrm{I,II}) < P_1(6s+r)[(2s+1+b)(s+a)q^{2s+1+b}] \tag{65}$$

and

$$\varepsilon_{i,j}(\mathrm{II,II}) < P_2(6s+r)[(2s+1+b)(s+a)q^{2s+1+b}] \tag{66}$$

Also for $i<j$ sufficiently far apart overlapping will be negligible and in those cases the probability that both i and j have a failure configuration occurring, $\varepsilon^*_{i,j}$, satisfies

$$\varepsilon^*_{i,j} < P_i(6s+r)P_j(6s+r), \quad i,j=1,2. \tag{67}$$

In fact there are fewer than $(6s+3+r)$ such cases [see Eq. (62)]. Thus letting

$$\varepsilon'_i = \sum_{\substack{j \in J_i \\ j \neq i}} E[Y_i Y_j], \tag{68a}$$

and taking account of all possible positions of fiber j in J_i, and noting $P(k)=P_1(k)+P_2(k)$, we sum $\varepsilon_{i,j}$, $\varepsilon_{j,i}$, $\varepsilon^*_{i,j}$, and $\varepsilon^*_{j,i}$ (because the positions of fibers i and j can be interchanged in the above discussion) to get

$$\varepsilon'_i \leqslant 4(6s+3+r)[(2s+1+b)(s+a)q^{2s+1+b}P(6s+r)] + 2(6s+3+r)P(6s+r)^2. \tag{68b}$$

It turns out that this bound suffices also for fiber i near the boundaries, where there are approximately only $6s$ such fibers whose dominant configurations are affected. Thus we can write

$$b_2 = \sum_{i=1}^{n} \varepsilon'_i \leqslant 4n(6s+3+r) \times [(2s+1+b)(s+a)q^{2s+1+b}P(6s+r)] + 2n(6s+3+r)P(6s+r)^2. \tag{69a}$$

Note that in doing the above calculations, the reason for the leftmost terminal ''1'' in defining our configurations becomes clear; without it the overlapping possibilities explode, yielding bounds of the same order as the probability, $G_n(x)$, being estimated, which are clearly of little value.

Lastly, we consider b_1 and b_3 in the Chen-Stein theorem presented in Appendix B. Clearly $b_3=0$ because the neighborhood J_i was constructed to ensure that any Y_j outside the neighborhood would be independent of Y_i. For b_1 we see that

$$b_1 \leqslant \sum_{i=1}^{n} \sum_{j \in J_i} E[Y_i]E[Y_j] \leqslant 2n(6s+3+r)P(6s+r)^2. \tag{69b}$$

Finally we sum b_1, b_2, and b_3, and calculate the error estimate (not counting the possible occurrence of *negligible* configurations associated with E_i)

$$\begin{aligned} \varepsilon_n &\equiv b_1+b_2+b_3 \leqslant 10n(6s+3+r) \\ &\quad \times[(2s+1+b)(s+a)q^{2s+1+b}P(6s+r)] \\ &= O(ns^3q^{2s+1+b})P(6s+r), \end{aligned} \tag{70}$$

where we have used the fact that $P(6s+r)<2(2s+1+b)(s+a)q^{2s+1+b}$ for s sufficiently large, as is checked through study of Eqs. (47) and (48).

In summary, in view of Eqs. (49), (51), (56), (59), (60) and (70), we have established a key result, namely

$$\begin{aligned} G_n(x) &= \{1-\exp[-nP(6s+r)]\}[1+O(1/s)] \\ &= \{1-\exp[-n\Lambda(6s+r)]\}[1+O(1/s)], \end{aligned} \tag{71}$$

where $s=s(x)$ and $r=r(x)$ are related to x by Eq. (15). A main idea in what follows is that as the bundle size n becomes large, so must s and k to keep the probability of failure, $G_n(x)$ roughly fixed. This will mean that x must become smaller and smaller, approaching zero. A crucial fact will be that these error and remainder terms will vanish in magnitude compared to the probability of failure $G_n(x)$ regardless of its magnitude.

IX. THE SIZE EFFECT AND RATE OF CONVERGENCE AS $n \to \infty$

Here we use the results of Sec. VII to determine the eventual size effect for composite strength as $n \to \infty$, paying strict attention to the decay of error terms. Recall from Eq. (49) that $P(k)=\Lambda(k)\{1+O(1/s)\}$, where $k=6s+r$, and $r=1,\ldots,6$. From Eq. (51) we rewrite $\Lambda(k)$ as

$$\Lambda(6s+r)=2s^2\Phi(s)\Theta(r)=s^2(q^2\delta)^s\Pi(r), \tag{72}$$

where

$$\Pi(r)=2\Theta(r)p^5\left(\frac{\delta}{\delta+2p}\right)^2\left(\frac{\delta}{q}\right). \tag{73}$$

From Eq. (71) the probability of failure of a large bundle under load x is

$$G_n(x) \approx 1-\exp[-nP(k)] \approx 1-\exp[-n\Lambda(6s+r)], \tag{74}$$

where we recall the relationships $s=\lceil 1/x \rfloor -1$, $k=\lceil 6/x \rfloor -6+1$, and $r=k-6s$ of Eq. (15).

To see the effects of bundle size n on the various error estimates in terms of s, we fix a probability level of bundle failure $0<\overline{P}<1$ and integer $1 \leqslant r \leqslant 6$, and from Eqs. (72) and (74) seek to invert

$$ns^2(q^2\delta)^s\Pi(r)=-\log(1-\overline{P}) \tag{75}$$

to get $s_n=s_n(r,\overline{P})$. Using results in Appendix C we get

$$\begin{aligned} \overline{s_n}(r,\overline{P}) = -\frac{1}{\log(q^2\delta)}\{&\log n+2\log\log n \\ &-2\log[-\log(q^2\delta)]-\log[-\log(1-\overline{P})] \\ &+\log\Pi(r)\}+o(1). \end{aligned} \tag{76}$$

For n above some small threshold value, these values of $\overline{s_n}$ form an increasing sequence in n but are not integers. For large n, taking the integer part $s_n=\lfloor \overline{s_n} \rfloor$ corresponds to the load region $k=6s_n+r$ which gives a higher probability of bundle failure than $\overline{P}$, and taking the next highest integer s_n+1 gives a load region $k=6(s_n+1)+r$ corresponding to a lower probability of failure. Note that by adjusting r, we can adjust k amongst its 12 possible values here to obtain two consecutive load regions, k' and $k'+1$, whose probabilities bracket $\overline{P}$, but it is not generally possible to solve for an exact load x given $\overline{P}$ because the bundle strength distribution is discrete.

Nevertheless, the effect of bundle size n is easily seen. Using the fact that $-\log(1-\overline{P})$ is approximately $\overline{P}$ we can interpret Eq. (76) as

$$s_n=O\left[-\frac{\log(n/\overline{P})}{\log(q^2\delta)}\right]. \tag{77}$$

Also, it can be shown that the size effect in bundle strength, X_n, is such that

$$X_n \log n \to -\log(q^2\delta) \tag{78a}$$

in probability as $n \to \infty$, or

$$\text{failure load} \sim \frac{-\log(q^2\delta)}{\log n}, \tag{78b}$$

being asymptotically true no matter what the value of $\overline{P}$. To see this note that as n grows large, the loads x in the corresponding load spans s_n or s_n+1 are all $(1/s_n)[1+O(1/s_n)]$ and the choice of $\overline{P}$ has a negligible effect on this value, even in relative terms. It turns out that the coefficient of variation in strength (standard deviation divided by the mean) also goes to zero as $n \to \infty$.

Returning to the Chen-Stein theorem, we are now in a position to evaluate the magnitudes of the various error terms as n grows large. In Eq. (59) we see from Eqs. (72), (75), and (77) that

$$\varepsilon_{E,n}=\left(\frac{n}{s_n}\right)P(k)=n\Lambda(6s_n+r)\left(\frac{1}{s_n}\right)\left[1+O\left(\frac{1}{s_n}\right)\right]$$
$$=O\left[\frac{\overline{P}}{\log(n/\overline{P})}\right]. \tag{79}$$

Similarly, for b_1

$$b_1\leqslant 2\left(\frac{1}{n}\right)(6s_n+3+r)[nP(6s_n+r)]^2=O\left[\frac{\overline{P}^2\log(n/\overline{P})}{n}\right]. \tag{80}$$

For b_2 we note that

$$b_2\leqslant 4(6s_n+3+r)[(2s_n+1+b)(s_n+a)q^{2s_n+1+b}$$
$$\times nP(6s_n+r)]+2(6s_n+3+r)[nP(6s_n+r)]^2, \tag{81}$$

but

$$(s_n)^3q^{2s_n}=O\left\{\frac{[\log(n/\overline{P})]^2}{(n/\overline{P})^{-2\log q}}\right\}, \tag{82}$$

and the second term is given already by Eq. (80) so

$$b_2=O\left\{\frac{\overline{P}[\log(n/\overline{P})]^2}{(n/\overline{P})^{-2\log q}}\right\}. \tag{83}$$

These error terms all go to zero as $n\to\infty$, but also important is the fact that they are proportional to the probability level $\overline{P}$. The error of approximation in Eq. (60) is ε_n which according to Eq. (70) is $b_1+b_2+b_3$. In view of Eqs. (80) and (83) and the fact that $b_3=0$, the error ε_n decreases not only in absolute terms (it is uniformly bounded in $\overline{P}$) but in terms relative to the probability level $\overline{P}$ of interest (also uniformly). That is, the error divided by the probability of interest, $\varepsilon/\overline{P}$, can be made arbitrarily small for $n>n_\varepsilon$, *independent of* $\overline{P}$, no matter how small.

We have neglected boundary effects in this discussion. The number of fibers affected, however, is approximately $6s$ out of n, which is $O[\log(n/\overline{P})]$. So in the above approximations, the error is about the same as that introduced by changing n by $O[\log(n/\overline{P})]$, and this makes no substantial difference in the asymptotics (as can be seen also by replacing n by $n-s_n$ in the derivations). As a practical matter, to avoid boundary effects we want

$$n\gg\frac{-6\log(n/\overline{P})}{\log(q^2\delta)}. \tag{84}$$

X. APPROXIMATIONS FOR THE PROBABILITY OF FAILURE OF LARGE BUNDLES AT LOW LOADS

Since we know how the error terms are structured in s, we seek to develop simple but accurate approximations to the distribution function $G_n(x)$ for bundle strength. This task is complicated by the fact that, as k increases, $\Lambda(k)$ of Eq. (51) has a factor $\Theta(r)$ of Eq. (50) that imparts quasiperiodic behavior in k as $k=6s+r$ changes with r through 1 to 6 for each value of s. To bound this periodicity recall that $s=\lceil 1/x\rceil-1$. Then careful inspection of the structure of $\Lambda(k)$ given by Eqs. (50) and (51) shows that a lower bound is

$$\Lambda_l(x)=2\left(\frac{1}{x}\right)^2q^{2[(1/x)-1]-1}\delta^{(1/x)-1+3}\frac{p^5}{(\delta+2p)^2}\Theta(1)$$
$$=2\left(\frac{1}{x}\right)^2q^{2/x}\delta^{1/x}\left(\frac{\delta}{\delta+2p}\right)^2\left(\frac{p^5}{q^3}\right)\Theta(1). \tag{85}$$

Except when $x=1/(1+s)$, $s=1,2,3,\ldots$, which occurs at the beginning of load span s [whereby $r=1$, so that $\Theta(1)$ applies] this approximation asymptotically (large s) yields an underestimate of the probability of failure. The maximum underestimate is by the factor $q\Theta(1)/\Theta(2)$. Thus we let

$$\Lambda_u(x)=\frac{\Theta(2)}{q\Theta(1)}\Lambda_l[k(x)]$$
$$=2\left(\frac{1}{x}\right)^2q^{2/x}\delta^{1/x}\left(\frac{\delta}{\delta+2p}\right)^2\left(\frac{p^5}{q^4}\right)\Theta(2). \tag{86}$$

We can then write

$$\Lambda[k(x)]=\left(\frac{1}{x}\right)^2(q^2\delta)^{1/x}\Pi^*(q)\Delta(1/x), \tag{87}$$

where

$$\Pi^*(q)=2\left(\frac{\delta}{\delta+2p}\right)^2\left(\frac{p^5}{q^4}\right)\Theta(2), \tag{88}$$

and

$$\Delta(1/x)=(x\lceil 1/x\rceil-x)^2(q^2\delta)^{\lceil 1/x\rceil-1/x}\left\{\frac{q\Theta[r(x)]}{\Theta(2)}\right\}, \tag{89}$$

where we recall from Eq. (15c) that $r(x)=k(x)-6s(x)=\lceil 6/x\rceil-6\lceil 1/x\rceil+1$. Note that $\Delta(1/x)$ is asymptotically (as $x\to 0^+$) periodic in $1/x$, varying between 1 and $q\Theta(1)/\Theta(2)$ with period 1, corresponding to integer increases in s.

A. Approximation for bundle strength distribution for large n and small x, and some numerical results

In view of Eq. (71) and Eqs. (87) to (89) our main asymptotic result is

$$G_n(x)\approx 1-\exp\left[-n\left(\frac{1}{x}\right)^2(q^2\delta)^{1/x}\Pi^*(q)\Delta(1/x)\right], \tag{90}$$

where we find that the *relative* error [absolute error divided by $G_n(x)$] is $O(x)$, which follows directly from Eq. (71).

In Fig. 5 we have plotted $\Lambda[k(x)]$ versus x for $q=0.05$ and for the range of x defined by $s=0,1$ (i.e., $0.333<x<1$) and $r=1,2,\ldots,6$. The dependence of k, r, and s on x is given by Eq. (15). This figure shows the discrete, ''step'' behavior of $\Lambda[k(x)]$ where the periodic feature is noticeable. A similar result is shown in Fig. 6 for the range of x defined by $s=12$ (i.e., $0.0714<x<0.0769$) and for $q=0.1$ and 0.2.

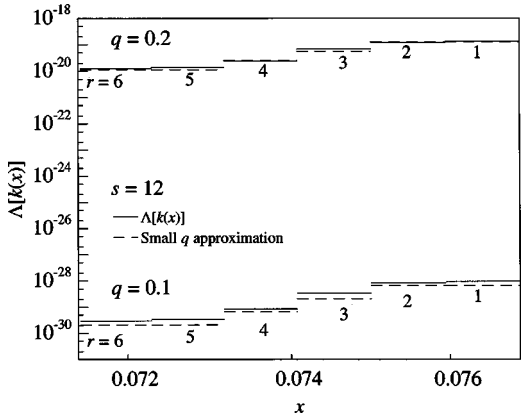

FIG. 6. Plot of $\Lambda[k(x)]$ versus x for $q=0.1$, 0.2 for the range $s=12$, and $r=1,2,\ldots,6$, and where $k=6s+r$ where the dependence of k, r, and s on x is given by Eq. (15). Also shown is the small q approximation (52), (53a), (53b), (87), and (88) where $\delta \approx \sqrt{q}+q/2$. The probability of failure of a bundle of n fibers is $G_n(x)\approx 1-\exp\{-n\Lambda[k(x)]\}$.

Also shown is the small q approximation Eqs. (52), (53a), (53b), (87), and (88) where $\delta\approx\sqrt{q}+q/2$.

We note that s of the order of 12 is necessary to develop a fairly full set of type I and type II failure configurations, as described in Sec. V. Note that the probability of failure of a bundle of n fibers is $G_n(x)\approx 1-\exp\{-n\Lambda[k(x)]\}$, so n must be of the order of $1/\Lambda[k(x)]$ to have a significant probability of failure. For $q=0.2$ and $s=12$, Fig. 6 shows that such configurations would not be observable by Monte Carlo simulation since $n>10^{18}$. One can check from Eq. (90) that only when q is significantly greater than 0.5 will such configurations readily occur.

The size effect is also easily obtained from Eq. (90). Setting the quantity inside the exponential of Eq. (90) equal to one and solving for x yields the characteristic strength x_n^*. We find that

$$x_n^* \sim \frac{-\log(q^2\delta)}{\log[\Pi^*(q)n](1+\alpha_n)}, \tag{91a}$$

as $n\to\infty$ where

$$\alpha_n=\frac{2\{\log\log[\Pi^*(q)n]-\log[-\log(q^2\delta)]\}}{\log[\Pi^*(q)n]-2}. \tag{91b}$$

We note that the correction term α_n, while decaying to zero as $n\to\infty$, does so very slowly, and thus cannot be ignored. This again points to a difficulty in using Monte Carlo simulation alone to establish the eventual size scaling, since the bundles would have to be extremely large to fully subdue the error term α_n. It can be shown that the coefficient of variation (c.o.v.) also decreases as $1/\log n$.

B. Approximation for distribution function for load at first fiber failure

The analysis for the *first fiber to fail* is similar to that for complete failure under LLS ($\theta=1$) as described in Harlow and Phoenix [41], but with a few modifications. For example, the most important configurations in TLS involve isolated ''1''s under $K_i^*=1+i/2$, where i is the number of adjacent neighbors, but the configuration ''1 1 0$\cdots$0'' with i contiguous ''0''s will not necessarily cause failure under $K_{i,0}x$ since $K_{i,0}<K_i^*$. Thus configurations where the first fiber to fail is one of the fibers in a crack arrestor pair require $i'=3i/2$ breaks, i.e., $i/2$ extra breaks as compared to an isolated ''1.'' Nevertheless, the same asymptotic results as in Harlow and Phoenix occur, though with slightly different error estimates. Thus an approximation can be developed for the distribution function for the bundle load when the *first* fiber fails. This distribution turns out to be

$$G_n^{(1)}(x)\approx 1-\exp\left[-n\left(\frac{2}{x}\right)q^{2/x}(p/q)^2\Delta^{(1)}(2/x)\right], \tag{92}$$

where

$$\Delta^{(1)}(2/x)=(\lceil 2/x\rceil x/2-x)q^{\lceil 2/x\rceil-2/x+1}. \tag{93}$$

Note that $\Delta^{(1)}(2/x)$ is asymptotically (as $x\to 0^+$) periodic in $2/x$, varying between 1 and q with period 1. In this case the characteristic load at first fiber failure, $x_n^{(1)*}$ decreases as

$$x_n^{(1)*}\sim -2\log q/\log n \tag{94}$$

[where we have not calculated the small correction term as in Eq. (91b)]. Also the c.o.v. varies as $1/\log n$. Clearly $x_n^{(1)*}$ scales differently form x_n^* given by Eqs. (91a) and (91b).

XI. DISCUSSION AND EXTENSIONS

A. Some extensions

The above analysis can be extended to a quasi-two-dimensional material structure in the form of a chain of m independent bundles with n fibers each. The analysis is the same upon replacing n by mn except that the boundary conditions need to be handled with some care. In the asymptotics we must let m and n grow large simultaneously noting that boundary effects will dominate unless

$$n\gg\frac{-6\log(mn/\overline{P})}{\log(q^2\delta)} \tag{95}$$

and a sufficient condition is $m\to\infty$ and $n\to\infty$ such that $(\log m)/n\to 0$. The physical meaning is that the bundle size n remains much larger than the longest local failure configuration in the material for a desired probability level $\overline{P}$.

Other types of boundary conditions are possible. The above analysis applies with more accuracy for circular bundles and chains thereof, and for spiral boundary conditions, but again, the above condition Eq. (95) must be satisfied. We also could have modified the load-sharing rule at the boundaries to prevent losing load at the edges by reflecting it back to the interior, but this strongly affects the boundary configurations at the very edges. The probabilities for certain failure configurations occurring for these boundary fibers would increase since, at the very edge, initiation and catastrophic failure configurations need to be about half as

long as those for the interior to cause failure. But the initiation has to be at the boundary for this to occur so the fraction of configurations involved is of order $1/s$ for larger s (small loads x, large bundles, n) compared to edge configurations in the previous case, and the probability for each is of order $(q^2\delta)^{s/2}$ roughly the square root of that for interior fiber positions. A straightforward calculation shows that n should be large compared to $(m/\overline{P})/[\log(mn/\overline{P})]^2$ for such boundary effects to be negligible.

Our analysis thus far has applied to bundles with $\theta=2/3$ in the tapered load-sharing rule. However, one can in principle apply the same procedure to any value of θ in the range $2/3\leqslant\theta<1$. For example, for $\theta=3/4$ we still have $K_i^*=1+i/2$, but $K_{i,0}=1+3i/8$ and $K_{0,i}=1+i/8$. But since 3 does not divide 8, we actually need a load span of $r=1,\ldots,12$ steps instead of 8 to obtain a repetitive pattern. The basic ideas all carry through (albeit tediously), and one obtains results of similar structure. In particular, for $\theta=3/4$, one has for a given probability of failure $\overline{P}$ roughly

$$\text{strength}\approx-\frac{\log(q^2\delta^{2/3})}{\log(n/\overline{P})}. \tag{96}$$

For general $2/3\leqslant\theta<1$ we conjecture

$$\text{strength}\approx-\frac{\log(q^2\delta^{2/\theta-2})}{\log(n/\overline{P})}. \tag{97}$$

In Sec. II, we discussed the characteristics of load redistribution in a model of Hedgepeth. One aspect was that next to break clusters of size t, load is redistributed beyond next nearest neighbors in decreasing amounts in distance z (varying as $1/\sqrt{z}$ for large t) and also that the load on the fiber adjacent to a cluster of t breaks does not grow linearly in t but rather as $\sim\sqrt{\pi t}/2$. It should be possible to generalize the tapered load-sharing scheme to such situations where load is shifted also to third-nearest neighbors, and so on. In this case failure might proceed through the existence of a crack initiation core of $s_0(x)$ ''0''s possibly interrupted by one ''1,'' then through a sequence of $s_1(x)$ fibers with no ''1 1''s adjacent, followed by propagation through a sequence of $s_2(x)$ fibers with no ''1 1 1''s, and so on. One envisions solving a sequence of eigenvalue problems for $\delta_1,\delta_2,\ldots$. Since the nearest neighbor overload factor is roughly $\sqrt{\pi t}/2$, ultimate breakdown may require a total string length of $s_0(x)+s_1(x)+\cdots+s_{l(x)}(x)\approx(4/\pi)/x^2$. Thus strength may decrease as some function $C(n/\overline{P},q,\delta_1,\delta_2,\ldots\delta_{l(x)})/(\log n)^{1/2}$. However, the nature of C is likely to be more complicated than suggested by formulas given in the Introduction (as suggested below for the first fiber to fail).

The analysis for the *first fiber to fail* is similar to that for complete failure under local load-sharing ($\theta=1$). The size effect result was that strength decreased as $-2\log q/[\log(n/\overline{P})]$. On the other hand, our results for Hedgepeth load sharing, Eq. (10), suggested that a long string of v ''0'' s interrupted by a single ''1'' in the middle has load $(\pi/2)v/\log v$ on it. In Appendix C we show that this leads to the size effect for the bundle load at first fiber failure, which is

$$x_n^{(1)*}\approx\frac{2}{\pi}\frac{\log q\,\log\log(n/\overline{P})}{\log(n/\overline{P})}, \tag{98}$$

which differs from the form Eq. (5) given in the Introduction or Eq. (94) for TLS. In addition, Eq. (10) also indicates that this load concentration factor holds approximately for isolated fibers in a neighborhood of width perhaps proportional to v around the center fiber. This leads to a distribution for the first fiber to fail, namely Eq. (92) modified perhaps to

$$G_n^{(1)}(x)\approx1-\exp\left[-nC^*(q,x)\log\left(\frac{1}{x}\right)\left(\frac{1}{x}\right)^{1+(\log q)/x}\right], \tag{99}$$

where $C^*(q,x)$ is a positive function bounded from below and above as $x\to0$. Again this form is more complicated than Eq. (4) or Eq. (92) for TLS. These are issues to pursue in future work.

B. Discussion

Comparing with results quoted in Sec I, we first compare the distributions $G_n^{(1)}(x)$ in Eq. (92) to $F(V_1)$ in Eq. (4) for first fiber failure. Since $q^{2/x}=\exp[-2\log(1-p)(-1/x)]$ and $\alpha_1\approx1$, the structure is similar except our result has the prefactor $(1/x)$ to this exponential. As just mentioned the size effect results Eqs. (94) and (5) are the same, both having inverse dependence on the log of the volume, but we also discussed the plausibility of a size effect following $(\log\log n)/\log n$ in Eq. (98) through analysis of a more accurate model. This all points to the pitfalls in using simple arguments.

A comparison of $G_n(x)$ of Eq. (90) to $F(V_b)$ in Eq. (4), is carried out upon noting that $(q^2\delta)^{1/x}=\exp[-\log(q^2\delta)(-1/x)]$, and because $\log(q^2\delta)$ does not have the same behavior in $q=1-p$ as $-\log(1-p)$, we have an immediate difference in the dependence of the constants on p. This difference stems from the fact that the most critical local breakdown configurations are not contiguous strings of breaks but rather extended strings with interrupting survivors especially near the fringes. This led earlier to determining an eigenvalue δ from a special recursion discussed in Appendix A. Beyond our idealization, the more realistic Hedgepeth model in Sec. II indicates that such a feature will persist in more complex models. Second, the factor α_b, in Eqs. (4) and (5), is about 1/2, whereas in our analysis the corresponding exponent is 1. This difference comes from assumptions on how the load at the edge of a long strings of ''0''s scales with its length, and as mentioned, our model would suggest the same exponent, 1/2, if we crudely used Hedgepeth load redistribution, Eq. (8), showing dependence on the *square* of the applied load. But we caution that use of a more realistic stress analysis is likely to introduce further complications. As discussed in Sec. II, it is possible for an ''extended'' failure configuration consisting of a central cluster with a series of broken and unbroken fibers at both its tips to be more detri-

mental than a central crack involving the same number of breaks. Proper treatment of this situation will change the factors $\log(q^2\delta)$ and $(1/x)^2$ in Eq. (90) and possibly the size effect Eqs. (91a) and (91b) to more complicated quantities (the first involving perhaps an unbounded number of eigenvalues).

If one were to perform Monte Carlo simulation on this system, it is interesting to ask what bundle size n would be needed for the asymptotic results to firmly dominate the behavior. As was mentioned in Sec. IV, $P(k)$ up to $k=12$ (the end of span $s=1$) does not yet reveal the impact of the eigenvalue δ which is $q^{1/2}$ for small q. Reviewing the derivations in Secs. V, VI, and VII shows that the leading s^2 behavior and the domination of the eigenvalue structure for all the dominant configurations does not really emerge until $s\approx 8$, which corresponds to loads $x<1/6$. From Eq. (77), for a probability of failure for a bundle of $\overline{P}$ we can see that the size of the bundle involved is

$$n\approx \overline{P}/[\Pi^*(q)s^2(q^2\delta)^s]. \tag{100}$$

For $\overline{P}=1/2$, $s=8$, $q=1/4$ (one in four elements is initially a ''0''), we get from Eq. (A3) $\delta=0.593$, and from Eqs. (88), (53a), and (53b) $\Pi^*(q)$ is roughly 2.5, so $n\approx 3.4\times 10^6$. This is a large bundle from a simulation point of view if one is to do many Monte Carlo replications. Thus the large size scale behavior is difficult to access through simulation alone. This situation worsens very quickly as q becomes smaller. In some sense this situation is a manifestation of the Petersburg paradox [61,62] in that an actual material of huge size—say 10^{14} elements—will show behavior not accessible by current computer technology and algorithms for simulation.

Finally, in studying microstructure-property relationships for strength and toughness in heterogeneous ceramics, Curtin [8] used a Monte Carlo model to study the statistical aspect of crack growth by introducing a large crack and watching it grow to instability under increasing load. He found that materials exhibit lower strength, toughness and reliability, than anticipated from continuum models of crack bridging based on local average properties. Though our model does not introduce a crack artificially but rather allows one to initiate naturally and grow, our conclusion is basically the same: Fracture initiation and propagation is difficult to capture through simplifying arguments because they neglect extreme events.

ACKNOWLEDGMENTS

S.L.P. acknowledges financial support from the National Science Foundation (CMS-9800413) and from the National Institute of Standards and Technology (PO No. 43SBN867130). I.J.B. acknowledges support from Los Alamos National Laboratory.

APPENDIX A: PROBABILITIES FOR FIBER SEQUENCES WITH NO ADJACENT ''1''s

Recall that X···X is a sequence of ''0''s and ''1''s such that no two 1's are adjacent, and let $\mathcal{X}_u=P_u\{\mathrm{X}\cdots\mathrm{X}\}$ be the initial probability of occurrence of such a sequence of length u. Inspection shows that all such configurations, can be generated by adding a ''0'' to the right end of those of length $u-1$, or a ''0 1'' to the right of those of length $u-2$. Thus one may write the recursion

$$\mathcal{X}_u=q\mathcal{X}_{u-1}+pq\mathcal{X}_{u-2}, \quad u\geqslant 2, \tag{A1}$$

with initial conditions $\mathcal{X}_0=\mathcal{X}_1=1$. Thus $\mathcal{X}_2=1-p^2$, and we add the natural extension $\mathcal{X}_{-1}=1/q$. A solution of the form $\mathcal{X}_u=C\delta^u$ yields the characteristic equation

$$\delta^2-q\delta+qp=0 \tag{A2}$$

with positive and negative roots

$$\delta=\frac{q+\sqrt{q^2+4pq}}{2}, \quad \delta^*=\frac{q-\sqrt{q^2+4pq}}{2}, \tag{A3}$$

where the first is largest in absolute value. Thus

$$\mathcal{X}_u=C_1\delta^u+C_2\delta^{*u}, \tag{A4}$$

where the initial conditions give $C_1+C_2=1$, and $C_1\delta+C_2\delta^*=1$, whose solution is

$$C_1=\frac{1-\delta^*}{\delta-\delta^*}, \quad C_2=\frac{\delta-1}{\delta-\delta^*}. \tag{A5}$$

Manipulating Eq. (A5) using $\delta+p=\delta^2/q$ from Eq. (A2), $\delta^*=q-\delta$ from Eq. (A3), and $p+q=1$, we obtain alternative relations for C_1 and C_2 so that Eqs. (A4) and (A5) combine to give

$$\mathcal{X}_u=\frac{\delta^2}{q^2}\left(\frac{\delta}{\delta+2p}\right)\delta^u+\frac{\delta^2}{q^2}\left(\frac{\delta}{\delta+2p}\right)\left(\frac{\delta-1}{\delta+p}\right)\delta^{*u}. \tag{A6}$$

Therefore, we have

$$P_u\{\mathrm{X}\cdots\mathrm{X}\}=\frac{\delta^2}{q^2}\left(\frac{\delta}{\delta+2p}\right)\delta^u\{1+\varepsilon_u\}, \tag{A7}$$

where

$$\varepsilon_u=(-1)^u\left(\frac{\delta-1}{\delta+p}\right)\left(\frac{\delta-q}{\delta}\right)^u\to 0 \quad \text{as } u\to\infty. \tag{A8}$$

Finally, considering $P_u\{\underline{\mathrm{X}}\cdots\underline{\mathrm{X}}\}$ and $P_u\{\mathrm{X}\cdots\underline{\mathrm{X}}\}$ where $\underline{\mathrm{X}}$ means that the terminal element on the side implied must be a ''0,'' we easily see that

$$P_u\{\underline{\mathrm{X}}\cdots\underline{\mathrm{X}}\}=qP_{u-1}\{\mathrm{X}\cdots\underline{\mathrm{X}}\}=q^2P_{u-2}\{\mathrm{X}\cdots\mathrm{X}\}. \tag{A9}$$

In particular, note the cases $P_1\{\underline{\mathrm{X}}\cdots\underline{\mathrm{X}}\}=q$ and $P_1\{\mathrm{X}\cdots\underline{\mathrm{X}}\}=q$. Finally we note that

$$P_u\{\underline{X}\cdots\underbrace{\underline{X}}^{v}\} = P_u\{\underline{X}\cdots\underline{X}\} - P_u\{\underline{X}\cdots\underline{X}\cap \text{ the last } v \text{ positions are all ``0''s}\} = P_u\{\underline{X}\cdots\underline{X}\} - P_{u-v}\{\underline{X}\cdots X\}q^v$$
$$= \left(\frac{\delta}{\delta+2p}\right)\delta^u\left[1+\varepsilon_{u-2}-\left(\frac{q}{\delta}\right)^{v-1}(1+\varepsilon_{u-v-1})\right]. \tag{A10}$$

APPENDIX B: CHEN-STEIN THEOREM

We give here a form of the Chen-Stein theorem following Barbour and Eagleson [59]. Let I be an arbitrary index set, and suppose that $\{Y_i, i\in I\}$ are 0 or 1 random variables with probabilities $p_i = P\{Y_i=1\} = 1-P\{Y_i=0\} = E[Y_i] > 0$. Also let $T_n = \Sigma_{i\in I} Y_i$ and $\lambda_n = E[T_n] = \Sigma_{i\in I} p_i$, and let W_n be a Poisson random variable with mean λ_n, where $\lambda_n \in (0,\infty)$. Let J_i denote an arbitrarily chosen set of ''near neighbors'' of i, and let $V_i = T_n - \Sigma_{j\in J_i} Y_j = \Sigma_{j\notin J_i} Y_j$. We think of J_i as a ''neighborhood of dependence'' for i, such that Y_i is independent or nearly independent of Y_j for $j\notin J_i$. Then for $A\subseteq Z_+$,

$$|P\{T_n\in A\} - P\{W_n\in A\}|$$
$$\leqslant \Delta f \sum_{i\in j}\sum_{j\in J_i} p_i p_j + \Delta f \sum_{i\in I}\sum_{\substack{j\in J_i \\ j\neq i}} E[Y_i Y_j]$$
$$+ \left|\sum_{i\in I} E\{(Y_i - p_i)\} f(V_i+1)\right| = b_1 + b_2 + b_3, \tag{B1}$$

where f is a particular function (depending on A) for which

$$\sup_x |f(x)| \leqslant 1, \quad \text{and} \quad \Delta f = \sup_x |f(x+1) - f(x)| \leqslant 1.$$

Loosely speaking, b_1 measures the size of the neighborhood of i, b_2 measures the expected number of events occurring in the neighborhood of a given event, and b_3 measures the dependence between the event Y_i and those occurring outside the neighborhood of i.

APPENDIX C: ASYMPTOTICS FOR LOAD x AT FIRST FIBER FAILURE

Suppose we have positive integers r and n, positive constant c, constant $0<q<1$, and integer φ with possible values $\varphi = -1,1,2$. Then the quantity

$$cr^{\varphi} q^r = \frac{1}{n} \tag{C1}$$

can be written as

$$[-\log(q^r)]^{\varphi} q^r = \frac{(-\log q)^{\varphi}}{cn}. \tag{C2}$$

As $n\to\infty$, this can be inverted to yield

$$r_n = -\frac{1}{\log q}[\log n + \varphi \log\log n - \varphi \log(-\log q) + \log c] + o(1) \tag{C3}$$

as can be verified by direct substitution.

Now suppose v is an integer, and

$$q^{-r} = v, \quad n = \frac{1}{x}, \quad \text{and} \quad \frac{-\log q}{c} = \frac{\pi}{2}. \tag{C4}$$

Then using Eq. (C1) with $\varphi = 1$, we have

$$\frac{v}{\log v} = \frac{2/\pi}{x} \tag{C5}$$

which using Eqs. (C2) and (C3) is inverted and exponentiated to give

$$v_x \sim \frac{2}{\pi}\left(\frac{1}{x}\right)\log\left(\frac{1}{x}\right). \tag{C6}$$

Next suppose

$$v q^v = \frac{\overline{P}}{n}, \tag{C7}$$

where p is a constant. Then using Eqs. (C1), (C3), and (C6) and keeping dominant terms we find that

$$\frac{x}{\log x} \sim \frac{2}{\pi}\frac{\log q}{\log(n/\overline{P})}, \tag{C8}$$

which inverts to give

$$x_n \sim \frac{2}{\pi}\frac{\log q \log\log(n/\overline{P})}{\log(n/\overline{P})}. \tag{C9}$$

[1] S. P. Timoshenko, *History of Strength of Materials* (McGraw-Hill, New York, 1953).

[2] Galileo Galilei, *Dialogues Concerning Two New Sciences (Italian and Latin)*, English translation by Henry Crew and Alfonso de Salvio (Macmillan, London, 1914) (reprinted by Dover, New York, 1952).

[3] W. Weibull, Proc. Royal Swedish Academy Eng. Sci. **151**, 1 (1939).

[4] W. Weibull, ASME J. Appl. Mech. **18**, 293 (1951).

[5] B. Epstein, J. Appl. Phys. **19**, 140 (1948).

[6] E. Castillo, *Extreme Value Theory in Engineering* (Academic, San Diego, 1988).

[7] A. M. Freudenthal, in *Fracture*, edited by Liebowitz (Academic, New York, 1968).
[8] W. A. Curtin, J. Am. Ceram. Soc. **78**, 1313 (1995).
[9] H. E. Daniels, Proc. R. Soc. London, Ser. A **183**, 405 (1945).
[10] D. E. Gücer and J. Gurland, J. Mech. Phys. Solids **10**, 365 (1962).
[11] R. L. Smith and S. L. Phoenix, ASME J. Appl. Mech. **103**, 75 (1981).
[12] B. D. Coleman, Trans. Soc. Rheol. **1**, 153 (1957).
[13] W. A. Curtin, J. Am. Ceram. Soc. **74**, 2837 (1991).
[14] S. L. Phoenix, M. Ibnabdeljalil, and C.-Y. Hui, Int. J. Solids Struct. **34**, 545 (1997).
[15] D. G. Harlow and S. L. Phoenix, J. Compos. Mater. **12**, 195 (1978).
[16] D. G. Harlow and S. L. Phoenix, J. Compos. Mater. **12**, 314 (1978).
[17] R. L. Smith, Proc. R. Soc. London, Ser. A **372**, 539 (1980).
[18] D. G. Harlow and S. L. Phoenix, Int. J. Fract. **17**, 601 (1981).
[19] R. L. Smith, S. L. Phoenix, M. R. Greenfield, R. B. Henstenburg and R. E. Pitt, Proc. R. Soc. London, Ser. A **388**, 353 (1983).
[20] R. L. Smith, Adv. Appl. Probab. **15**, 304 (1983).
[21] D. G. Harlow, Proc. R. Soc. London, Ser. A **397**, 211 (1985).
[22] C. C. Kuo and S. L. Phoenix, J. Appl. Probab. **24**, 137 (1987).
[23] S. L. Phoenix and I. J. Beyerlein, in *Comprehensive Composite Materials*, edited by A. Kelly and C. Zweben (Pergamon–Elsevier Science, New York, 2000), Vol. 1, Chap. 1.19.
[24] L. de Arcangelis, S. Redner, and H. J. Herrmann, J. Phys. (France) Lett. **46**, L585 (1985).
[25] L. de Arcangelis, S. Redner, and A. Coniglio, Phys. Rev. B **34**, 4656 (1986).
[26] B. Kahng, G. G. Batrouni, and S. Redner, J. Phys. A **20**, L827 (1987).
[27] P. M. Duxbury, P. L. Leath, and P. D. Beale, Phys. Rev. B **36**, 367 (1987).
[28] P. M. Duxbury and P. L. Leath, J. Phys. A **20**, L411 (1987).
[29] Y. S. Li and P. M. Duxbury, Phys. Rev. B **36**, 5411 (1987).
[30] S. Roux, A. Hansen, H. Herrmann, and E. Guyon, J. Stat. Phys. **52**, 237 (1988).
[31] Y. S. Li and P. M. Duxbury, Phys. Rev. B **40**, 4889 (1989).
[32] P. D. Beale and P. M. Duxbury, Phys. Rev. B **37**, 2785 (1988).
[33] S. G. Kim and P. M. Duxbury, J. Appl. Phys. **70**, 3164 (1991).
[34] P. L. Leath and W. Xia, Phys. Rev. B **44**, 9619 (1991).
[35] M. Sahimi and J. D. Goddard, Phys. Rev. B **33**, 7848 (1986).
[36] P. D. Beale and D. J. Srolovitz, Phys. Rev. B **37**, 5500 (1988).
[37] A. Hansen, S. Roux, and H. J. Herrmann, J. Phys. (France) **50**, 733 (1989).
[38] *Statistical Models for the Fracture of Disordered Media*, edited by H. J. Herrmann and S. Roux (North-Holland, Amsterdam, 1990).
[39] A. Hansen, in *Statistical Models for the Fracture of Disordered Media*, edited by H. J. Herrmann and S. Roux (North-Holland, Amsterdam, 1990).
[40] A. Hansen, E. L. Hinrichsen, and S. Roux, Phys. Rev. B **43**, 665 (1991).
[41] D. G. Harlow and S. L. Phoenix, J. Mech. Phys. Solids **39**, 173 (1991).
[42] P. M. Duxbury and P. L. Leath, Phys. Rev. B **49**, 12676 (1994).
[43] P. L. Leath and P. M. Duxbury, Phys. Rev. B **49**, 14905 (1994).
[44] P. M. Duxbury and P. L. Leath, Phys. Rev. Lett. **72**, 2805 (1994).
[45] S. D. Zhang and E. J. Ding, Phys. Lett. A **193**, 425 (1994).
[46] S. D. Zhang and E. J. Ding, J. Phys. A **28**, 4323 (1994).
[47] S. D. Zhang and E. J. Ding, Phys. Rev. B **53**, 646 (1996).
[48] M. Kloster, A. Hansen, and P. C. Hemmer, Phys. Rev. E **56**, 2615 (1997).
[49] W. A. Curtin and H. Scher, Phys. Rev. B **55**, 12038 (1997).
[50] W. A. Curtin and H. Scher, Phys. Rev. B **55**, 12051 (1997).
[51] W. I. Newman, A. M. Gabrielov, T. A. Durand, S. L. Phoenix, and D. L. Turcotte, Physica D **77**, 200 (1994).
[52] J. M. Hedgepeth, ''Stress Concentrations in Filamentary Structures,'' NASA TN D-882 (1961).
[53] W. B. Fichter, ''Stress Concentration Around Broken Filaments in a Filament-Stiffened Sheet,'' NASA TN D-5453 (1969).
[54] I. J. Beyerlein, S. L. Phoenix, and A. M. Sastry, Int. J. Solids Struct. **33**, 2543 (1996).
[55] I. J. Beyerlein and S. L. Phoenix, Eng. Fract. Mech. **57**, 241 (1997).
[56] I. J. Beyerlein and S. L. Phoenix, Eng. Fract. Mech. **57**, 267 (1997).
[57] F. Hikami and T. W. Chou, AIAA J. **28**, 499 (1990).
[58] R. Arratia, L. Goldstein, and L. Gordon, Stat. Sci. **5**, 403 (1990).
[59] A. D. Barbour and G. K. Eagleson, J. R. Stat. Soc. B **46**, 397 (1984).
[60] L. Gordon, M. F. Schilling, and M. S. Waterman, Prob. Theor. Relat. Fields **72**, 279 (1986).
[61] P. Palffy-Muhoray, R. Barrie, B. Bergersen, I. Carvalho, and M. Freeman, J. Stat. Phys. **55**, 119 (1984).
[62] P. Palffy-Muhoray, in *Lectures on Thermodynamics, and Statistical Mechanics*, edited by M. Lopéz de Haro and C. Varea (World Scientific, London, 1991).
[63] C. Hsieh and R. Thompson, J. Appl. Phys. **44**, 2051 (1973).
[64] S. J. Zhou and W. A. Curtin, Acta Metall. Mater. **43**, 3093 (1995).
[65] M. Ibnabdeljalil and W. A. Curtin, Int. J. Solids Struct. **34**, 2649 (1997).
[66] S. B. Batdorf, ASME J. Appl. Mech. **50**, 190 (1983).
[67] H. M. Taylor and D. E. Sweitzer, Adv. Appl. Probab. **30**, 342 (1998).
[68] H. M. Taylor, J. Appl. Probab. **36**, 1 (1999).
[69] H. M. Taylor (private communication).
[70] H. Kesten, Ill. J. Math. **5**, 267 (1961).